1-1-2013

Epigenetic Basis for the Oncogenic Potential of IDH Mutations

Chao Lu
University of Pennsylvania, jimmyluchao@gmail.com

Epigenetic Basis for the Oncogenic Potential of IDH Mutations

Abstract
Although many complex diseases including cancer manifest aberrant cellular metabolism and chromatin structure, the molecular connection between two processes remains poorly understood. The metabolite, α-ketoglurate (αKG), is a critical co-factor for a number of chromatin modifying enzymes. Its structural analogue, 2-hydroxyglutarate (2HG), was recently identified as the product of cancer-associated mutations in isocitrate dehydrogenases (IDH). To determine whether metabolic perturbation can disrupt chromatin remodeling and transcription, I investigated the epigenetic consequences of 2HG-producing IDH mutations. In this thesis, 2HG was demonstrated to be a competitive inhibitor for αKG-dependent chromatin modifiers including TET family DNA hydroxylases and jumonji-C histone demethylases. Expression of mutant IDH in cell lines led to global increases in histone and DNA methylation. In patient tumor samples, IDH mutations were tightly associated with DNA and histone hypermethylation and were mutually exclusive with loss of function mutations in TET2. Importantly, IDH mutation impaired cell differentiation which could be phenocopied by exogenous 2HG or depletion of 2HG-inhibitable TET2 or histone demethylase. Moreover, mutant IDH was sufficient for in vitro transformation and in vivo tumorigenesis and its malignant potential could be attributed to epigenetic gene silencing through DNA hypermethylation. Collectively, the data presented in this thesis provide insight into the tumorigenic mechanism by IDH mutations and suggest that both normal and neomorphic metabolite levels contribute to chromatin structure and transcriptional regulation.

Degree Type
Dissertation

Degree Name
Doctor of Philosophy (PhD)

Graduate Group
Cell & Molecular Biology

First Advisor
Craig B. Thompson

Second Advisor
Roger A. Greenberg

Keywords
2-hydroxyglutarate, Cancer, Cell differentiation, Epigenetic, Histone and DNA methylation, Isocitrate dehydrogenase mutation

Subject Categories
Biochemistry | Cell Biology | Oncology

EPIGENETIC BASIS FOR THE ONCOGENIC POTENTIAL OF IDH MUTATIONS

Chao Lu

A DISSERTATION

in

Cell and Molecular Biology

Presented to the Faculties of the University of Pennsylvania

in

Partial Fulfillment of the Requirements for the

Degree of Doctor of Philosophy

2013

Supervisor of Dissertation

_____

Craig B. Thompson, M.D.

Member, Sloan-Kettering Institute

Co-Supervisor of Dissertation

_____

Roger A. Greenberg, M.D., Ph.D.

Associate Professor of Cancer Biology

Graduate Group Chairperson

_____

Daniel S. Kessler, Ph.D., Associate Professor of Cell and Developmental Biology

Dissertation Committee

Constantinos Koumenis, Ph.D., Associate Professor of Radiation Oncology

Shelley L. Berger, Ph.D., Daniel S. Och University Professor

Martin Carroll, M.D., Associate Professor of Medicine

Gerd A. Blobel, M.D., Ph.D., Professor of Pediatrics

EPIGENETIC BASIS FOR THE ONCOGENIC POTENTIAL OF IDH MUTATIONS

Dedication

To my grandparents, who are always there to support and inspire me.

ACKNOWLEDGMENT

The work presented in this thesis would not be possible without invaluable help from many people. First I want to thank my thesis supervisor Craig Thompson for his support and guidance of my research. I also want to thank members of the Thompson lab, past and present, for technical, intellectual and moral help over the years. I particularly appreciate the mentorship from Katy Wellen, who also introduced me to the fascinating world of metabolism and epigenetics. I want to express my deepest gratitude to Patrick Ward, who pioneered in the research on IDH mutations and provided the foundation for my thesis work. Exchanging scientific ideas with him has always been extremely fruitful and I could never ask for a better colleague. I have been very fortunate to collaborate with many world-class scientists and I want to express my thanks to them: Ross Levine, Omar Abdel-Wahab, Timothy Chan, Ingo Mellinghoff, Ari Melnick, Lucy Godley and Donald O'Rourke. Lastly I want to thank the members of my thesis committee for their valuable scientific inputs and moral support: Constantinos Koumenis, Shelley Berger, Martin Carroll and Gerd Blobel. Thanks also to Roger Greenberg for graciously agreeing to serve as my co-supervisor.

ABSTRACT

EPIGENETIC BASIS FOR THE ONCOGENIC POTENTIAL OF IDH MUTATIONS

Chao Lu

Craig B. Thompson

Roger A. Greenberg

Although many complex diseases including cancer manifest aberrant cellular metabolism and chromatin structure, the molecular connection between two processes remains poorly understood. The metabolite, α-ketoglurate (αKG), is a critical co-factor for a number of chromatin modifying enzymes. Its structural analogue, 2-hydroxyglutarate (2HG), was recently identified as the product of cancer-associated mutations in isocitrate dehydrogenases (IDH). To determine whether metabolic perturbation can disrupt chromatin remodeling and transcription, I investigated the epigenetic consequences of 2HG-producing IDH mutations. In this thesis, 2HG was demonstrated to be a competitive inhibitor for αKG-dependent chromatin modifiers including TET family DNA hydroxylases and jumonji-C histone demethylases. Expression of mutant IDH in cell lines led to global increases in histone and DNA methylation. In patient tumor samples, IDH mutations were tightly associated with DNA and histone hypermethylation and were mutually exclusive with loss of function mutations in TET2. Importantly, IDH mutation impaired cell differentiation which could be phenocopied by exogenous 2HG or depletion of 2HG-inhibitable TET2 or histone demethylase. Moreover, mutant IDH was sufficient for *in vitro* transformation and *in vivo* tumorigenesis and its malignant potential could be

attributed to epigenetic gene silencing through DNA hypermethylation. Collectively, the data presented in this thesis provide insight into the tumorigenic mechanism by IDH mutations and suggest that both normal and neomorphic metabolite levels contribute to chromatin structure and transcriptional regulation.

TABLE OF CONTENTS

LIST OF FIGURES

Chapter 1

Introduction

Parts of this chapter have previously been published in: Lu C, Thompson CB. Metabolic regulation of epigenetics. *Cell Metab* 2012 16:9-17.

Metabolic regulation of epigenetics: a concept

Cells, whether as unicellular organisms or within a multicellular organism, need to make various "decisions" throughout their lifetime. Every choice—quiescence, proliferation, differentiation or migration—is made in the face of the constantly changing environment. Metazoan cells have developed elegant mechanisms to sense and integrate extracellular information into an intrinsic signaling system that regulates transcription so that variations in the form of growth factors, hormones, and stromal interactions can be registered and responded to in a timely and accurate manner. Studying these mechanisms remains a major focus of biological research and has profound implications in understanding human physiology and diseases.

One of the most exciting advances over the past 15 years is the field of epigenetics (meaning "above" genetics). We now know that in addition to primary DNA sequence information, much of the information regarding when and where to initiate transcription is stored in covalent modifications of DNA and its associated proteins. The patterns of various modifications along the chromatin, such as DNA cytosine methylation and hydroxymethylation, and acetylation, methylation, phosphorylation, ubiquitination, and SUMOylation of the lysine (K) and/or arginine (R) residues of histones are thought to regulate the genome accessibility to transcriptional machinery. For example, acetylation of histone lysine residues and methylation of H3K4, H3K36, and H3K79 are associated with active transcription while methylation of DNA, H3K9, H3K27, and H4K20 generally indicates silenced chromatin. In many instances, such information is heritable. The complexity and dynamics of epigenetic modifications are considered to provide a link between the extracellular environment and nuclear transcription. It is increasingly

appreciated that many growth factor/hormone-responsive signaling pathways such as Notch and TGFβ, often in conjunction with downstream transcription factors, can remodel the epigenome through expressing, recruiting or editing enzymes that modify chromatin (Mohammad and Baylin, 2010). One good example is the Notch effector RBP-J: depending on the presence of activated Notch, RBP-J recruits distinct histone-modifying enzymes to activate or repress target gene expression (Liefke et al., 2010).

A less studied but recently emerged concept is that information about a cell's metabolic state is also integrated into the regulation of epigenetics and transcription (Figure 1.1). It is now appreciated that cells constantly adjust their metabolic state in response to extracellular signaling and/or nutrient availability (Vander Heiden et al., 2009). As a classical example, while quiescent cells fully oxidize glucose to carbon dioxide in the mitochondrial electron transport chain; proliferative cells and tumor cells consume much larger quantities of glucose, secreting excess carbon as lactate even when oxygen is abundant, a process termed “aerobic glycolysis.” Connections between metabolism and transcription are not unexpected. As discussed later, in unicellular organisms like yeast the major determinant of cell fate is nutrient levels. Even in metazoans where most cellular signaling events are dictated by growth factors, cytokines or hormones, metabolism still plays a significant role in transcription. This also has a potentially unifying logic, as most chromatin-modifying enzymes require substrates or cofactors that are intermediates of cell metabolism. It is not difficult to imagine that fluctuation of metabolite levels could modulate the activities of chromatin-modifying enzymes and therefore influence chromatin dynamics. As many complex diseases such as cancer and type II diabetes display abnormalities of cellular metabolism and epigenome,

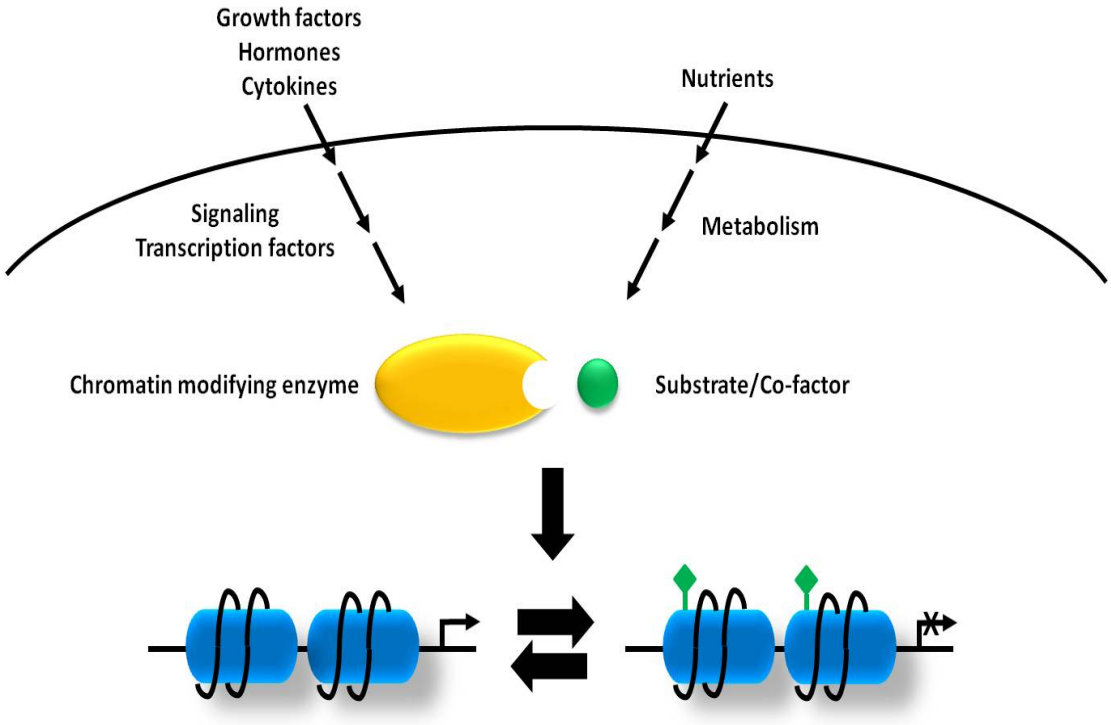

Figure 1.1: Signaling and metabolic inputs into epigenetics.

Growth factors, hormones and cytokines activate the classical signaling pathways and downstream transcriptional factors which will recruit chromatin-modifying enzymes to local chromatin. On the other hand, nutrient levels and cell metabolism will affect levels of the metabolites which are required substrates of chromatin-modifying enzymes that use these metabolites to post-translationally modify both histones and DNA. Variations in these two inputs will determine the epigenome remodeling and transcription.

understanding the molecular connections between these processes may have therapeutic implications.

Metabolites drive oscillatory gene expression in yeast

Most laboratory strains of budding yeast *Saccharomyces cerevisiae* are cultured in medium with abundant nutrients. As unicellular organisms, yeast under such conditions uptake extracellular nutrients avidly and exploit nutrient capture to fuel cell growth and proliferation at a logarithmic rate. However, under conditions where one or more nutrients are limiting, yeast tend to display oscillatory metabolic behavior with distinct phases characterized by robust changes in oxygen consumption (Chance et al., 1964). These metabolic oscillations can vary from minutes to hours depending on yeast strains and experimental conditions and are independent of cell division cycle (Slavov et al., 2011). Remarkably, when genome-wide gene expression in yeast under such culture system was analyzed, nearly 60% of the genes were expressed in a similarly cyclic fashion (Klevecz et al., 2004; Tu et al., 2005).

These data suggest that metabolite levels might be contributing to the temporal control of gene expression. This is supported by the observations that transient administration of metabolites, particularly the glycolytic intermediates, could initiate phase advancement in the oscillatory cycle (Cai et al., 2011; Tu and McKnight, 2009). Levels of acetyl-CoA, the product of glycolytic metabolism and a donor to histone acetylation reactions, were found to oscillate dynamically and peak during the oscillatory growth phase (Cai et al., 2011; Tu et al., 2007). Genome-wide analysis of H3K9 acetylation showed that its enrichment at genes expressed during growth phase correlated with acetyl-CoA levels

and was dependent on the generation of acetyl-CoA. Therefore it appears that levels of acetyl-CoA can be instructive for cells to engage growth at least in part through modulating histone acetylation and transcription of growth genes. Such a mechanism may well operate at other times. For example, the exit of yeast from quiescence has been reported to require glucose catabolism but not cell cycle signaling (Laporte et al., 2011).

Histone acetylation is responsive to glucose metabolism in human cancer cells

Unlike yeast, metazoan cells lack the autonomous ability to uptake and metabolize nutrients. Instead cellular nutrient uptake is under the control of a mixture of growth factor, paracrine and hormonal signaling. These factors control the positions that differentiated cells can survive in the body and dictate the share of the body's resources a cell can utilize in maintaining itself.

However, arguably the most fundamental hallmark of cancer cells is the sustained growth and proliferation which are independent of growth factors and hormones (Hanahan and Weinberg, 2011). This can be achieved through activating mutations and amplifications in the mitogenic signaling pathways (e.g. PI3K and RAS), and/or suppression of negative growth regulators (e.g. PTEN). As a result, similar to yeast cancer cells possess a constitutively active anabolic metabolism and avidly take up nutrients in the environment to ensure maximum growth and proliferation. This observation has been clinically applied as the use of positron-emission tomography (PET) to image the uptake of a glucose analogue ^{18}F-2-deoxyglucose by tumor cells (Vander Heiden et al., 2009). Moreover, before sufficient generation of tumor-associated neovasculature, cancer cells often experience dramatic variations in extracellular nutrient levels. Therefore it is

plausible that in cancer cells metabolic state may influence gene expression and cell behavior through the regulation of epigenetics. Consistent with this notion, compared to normal tissues tumors often show aberrant epigenome profiles which are thought to be critical for their initiation, progression and maintenance (Baylin and Jones, 2011).

A landmark paper by *Wellen et al*. confirmed the above hypothesis by demonstrating the link between glucose metabolism and histone acetylation in colon cancer cells (Wellen et al., 2009). In mammals, most cytosolic acetyl-CoA comes from citrate exported from mitochondria by a reaction catalyzed by ATP-citrate lyase (ACL) (Figure 1.2). *Wellen et al.* found that a fraction of ACL is localized in the nucleus and knocking down ACL substantially reduced the levels of histone acetylation. As a result, the expression of glucose metabolism genes was affected and cells with diminished ACL showed defects in growth, proliferation and differentiation. This study suggests that chromatin states are sensitive to the fluctuation of metabolite levels, which may represent an important mechanism for tumor cells to adapt to their microenvironment. However, it remains to be explored whether other metabolites in addition to acetyl-CoA contribute to regulatory events at the chromatin.

Histone and DNA demethylation are important chromatin events and require αKG

The methylation of 5' position of cytosines in DNA is probably the most studied epigenetic modification so far. In mammals, cytosine methylation occurs mainly at the CpG dinucleotides. Most CpG sites are present at repetitive elements of the genome and constitutively methylated, however they are also found at gene promoters as clusters known as "CpG islands". Importantly, while in normal tissues CpG islands are mostly not

methylated, tumor cells display hypermethylation at these sites (Baylin and Jones, 2011). DNA hypermethylation at gene promoters correlates with transcriptional repression and it is believed that DNA hypermethylation initiates/promotes tumorigenesis through silencing tumor-suppressor genes. Supporting this notion, inhibitors of DNA methyltransferases, the enzymes responsible for adding the methyl group to cytosines, are approved as anti-leukemia agents in clinic.

In addition to acetylation, histone lysine residues can also be methylated (Klose and Zhang, 2007). While histone acetylation generally correlates with transcriptional activation, histone methylation contributes to both transcriptional activation and repression. In general, methylation of H3K4, H3K36 and H3K79 indicates active chromatin while methylation of H3K9, H3K27 and H4K20 is associated with repressed chromatin. Moreover, each lysine residue can be modified into mono- (me1), di-(me2), or tri-(me3) methylated state. The complex patterns of histone methylation, together with acetylation and other modifications such as phosphorylation and SUMOylation, are thought to provide a so-called "histone code" to be recognized by specific "reader" proteins to initiate downstream chromatin remodeling events (Strahl and Allis, 2000). The role of histone methylation in cancer is poorly understood and likely to be tissue-specific.

A covalent methyl group is chemically stable. Therefore DNA and histone methylation were considered as relatively static epigenetic marks. However during embryonic development there is extensive remodeling of the cellular methylome, suggesting the existence of enzymes that actively remove methylation marks. Indeed in recent years, a variety of histone demethylases (HDMs) and DNA hydroxylases (DNHDs) have been identified. A family of HDMs named Jumonji-C domain containing HDM (JHDM) was

shown to remove methylation from histones through a reaction that utilizes αKG, oxygen and Fe (II) as co-factors and releases succinate and formaldehyde as by-products (Tsukada et al., 2006). Similar mechanism was adopted by the newly identified TET family enzymes that hydroxylate the 5-methylcytosine of DNA (Tahiliani et al., 2009). The only difference is that in this reaction, the hydroxymethyl group is a stable product and further TET-dependent modification is undertaken with low stoichiometry (He et al., 2011). The function of 5-hydroxymethylcytosine is the topic of intensive investigation and thought to serve as an intermediate for subsequent active (TET-dependent) or passive (replication-dependent) demethylation (He et al., 2011; Tahiliani et al., 2009). Notably, loss-of-function mutations in members of JHDM and TET families have been identified in various malignancies (Delhommeau et al., 2009; van Haaften et al., 2009).

From metabolic perspective, the demethylation mechanism by JHDMs and TETs is interesting as it requires αKG, a key metabolite in TCA cycle and a starting point for many anabolic pathways (Figure 1.2). αKG can be derived from glutamine through two deamination reactions; it is also an intermediate metabolite of glucose metabolism. Since glucose and glutamine are the two most abundant and important nutrients used by cells, it is plausible that αKG may be a critical messenger to relay information about nutrient state to chromatin through modulating the demethylation efficiency of histone and DNA demethylases.

IDH1 and IDH2 generate αKG and are recurrently mutated in cancer

αKG can be generated through the decarboxylation of isocitrate, a reaction catalyzed by IDH family enzymes. IDH family has three members: IDH1, IDH2 and IDH3. IDH3 is

known as the classical mitochondrial TCA cycle enzyme and its reaction utilizes NADH as co-factor. In contrast, IDH1 and IDH2 use NADPH as co-factor and are structurally very different from IDH3. The main distinction between IDH1 and IDH2 is their subcellular localization: IDH1 is mainly cytosolic and peroxisomal and IDH2 is a mitochondrial enzyme. The role of IDH1 and IDH2 in normal cell physiology is poorly understood.

Recently, cancer genome sequencing projects revealed unexpected recurring somatic mutations of IDH1 and IDH2 in ~70% intermediate-grade gliomas and ~20% of *de novo* acute myeloid leukemia (AML) (Mardis et al., 2009; Yan et al., 2009). Targeted sequencing in other tumor types also found their mutations in ~50% of central and periosteal cartilaginous tumors (Amary et al., 2011), ~30% intrahepatic cholangiocarcinomas (Borger et al., 2012), and ~20% angioimmunoblastic T-cell lymphoma (Cairns et al., 2012). IDH mutations found in above-mentioned cancers are always heterozygous and limited to R132 residue of IDH1 or R172 or R140 residues of IDH2. This strongly suggests that IDH mutations are not loss-of-function. Although it was originally proposed that mutant IDH1 acts as a dominant-negative enzyme (Zhao et al., 2009), unbiased metabolomic screening and enzymatic study showed that the mutation gives IDH1 a novel property to reduce αKG to 2-hydroxyglutarate (2HG) (Dang et al., 2009). This neomorphic enzyme activity was also shown with mutant IDH2 as well as less frequently observed IDH mutations in other types of cancer such as IDH1 G97D and IDH1 R100A mutations (Ward et al., 2012; Ward et al., 2010). Although 2HG is present in cells as a rare by-product from mitochondrial metabolism, patient samples with

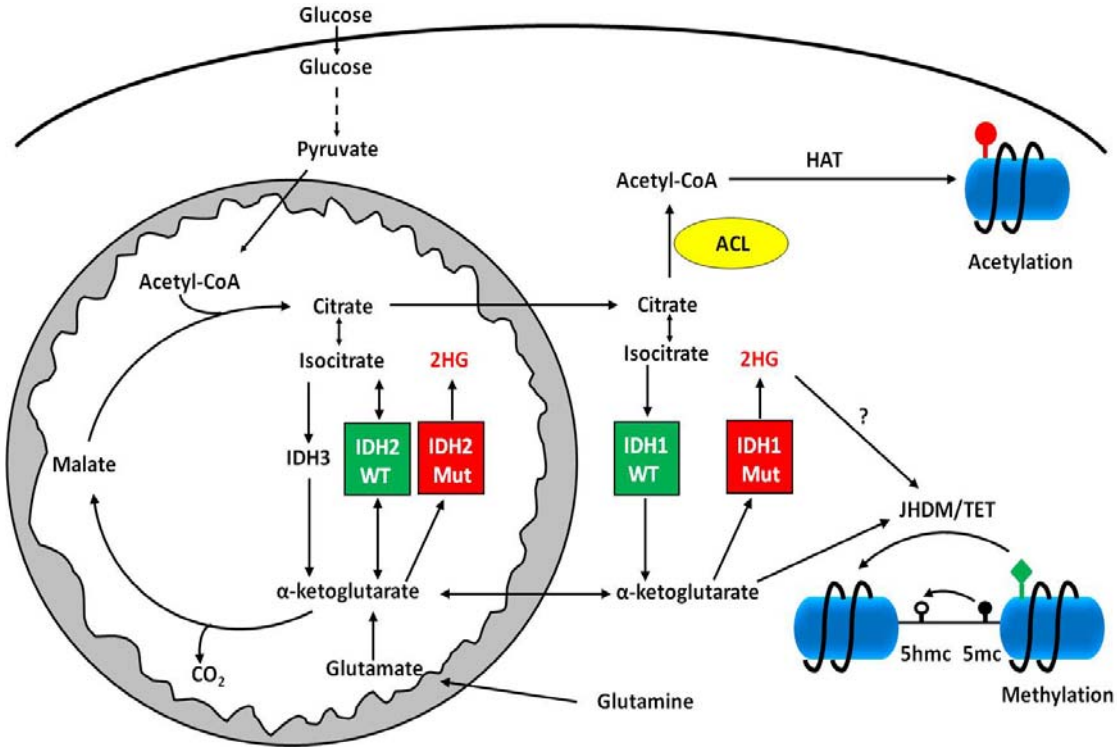

Figure 1.2: Crosstalk between metabolism and epigenetics in cancer.

In proliferative cells such as tumor cells, most citrate in the TCA cycle is exported to cytosol where it is catabolized to acetyl-CoA by the enzyme ACL. Acetyl-CoA generated by ACL can be used for the biosynthesis of lipid. They are also important donors for histone acetylation. Alternatively citrate can be converted to isocitrate, which is further metabolized to αKG by IDH1 in the cytosol and IDH2 in the mitochondria. Enzymes that remove the methylation from histone or DNA use αKG as co-factors. IDH1 and IDH2 were found to be frequently mutated in cancer. The mutation results in the accumulation of 2HG, a structural analogue of αKG. This thesis aims to investigate the impact of 2HG on chromatin methylation and tumorigenesis.

IDH mutations showed a 10-100 fold increases in 2HG accumulation, reaching absolute concentration as high as 10-50 mM (Dang et al., 2009). Of note, levels of αKG did not alter in tumors with IDH mutations.

Since the only difference between 2HG and αKG is that the α-keto group on αKG is replaced by the hydroxyl group on 2HG, the two metabolites are structurally similar. Hence 2HG-producing IDH mutations provide a great opportunity to investigate if perturbation of αKG homeostasis in cells is sensed by histone and DNA demethylation and leads to changes in gene expression and cell behavior. Moreover, the high frequencies of IDH mutations in multiple types of cancer strongly suggest that they are driver mutations; therefore this thesis also aims to determine whether IDH mutation is indeed oncogenic and the role of epigenetic dysregulation in its transformation process.

Chapter 2

Leukemic IDH1 and IDH2 mutations disrupt TET2 Function and result in DNA hypermethylation

Parts of this chapter have previously been published in: Figueroa ME, Abdel-Wahab O, Lu C, Ward PS, Patel J, Shih A, Li Y, Bhagwat N, Vasanthakumar A, Fernandez HF, Tallman MS, Sun Z, Wolniak K, Peeters JK, Liu W, Choe SE, Fantin VR, Paietta E, Löwenberg B, Licht JD, Godley LA, Delwel R, Valk PJ, Thompson CB, Levine RL, Melnick A. Leukemic IDH1 and IDH2 mutations result in a hypermethylation phenotype, disrupt TET2 function, and impair hematopoietic differentiation. *Cancer Cell* 2010 18:553-67.

Summary

Leukemia-associated IDH mutations are characterized by a neomorphic enzyme activity and resultant 2-hydroxyglutarate (2HG) production. Here we demonstrate that 2HG-producing mutant IDH1 and IDH2 inhibit TET2, an α-ketoglutarate-dependent DNA hydroxylases enzyme also mutated in acute myeloid leukemia (AML). Expression of IDH in myeloid cells decreased levels of 5-hydroxymethylcytosine and induced global DNA hypermethylation. In an AML patient cohort, IDH1/2 mutations were mutually exclusive with loss-of-function mutations in TET2. Furthermore, either expression of mutant IDH1/2 or Tet2 depletion increased stem/progenitor cell marker expression in hematopoietic cells, suggesting a shared pro-leukemogenic effect. This work identifies IDH1/2- and TET2-mutant leukemias as a biologically distinct disease subtype, and links cancer metabolism with epigenetic control of gene expression.

Introduction

Acute myeloid leukemia (AML) pathogenesis is characterized by recurrent chromosomal translocations and somatic mutations that can define biologically distinct disease subtypes. Among these abnormalities are mutations or rearrangement of genes encoding aberrant transcription factors or cofactors that directly perturb gene expression and disrupt cell differentiation and survival. Others include gain of function mutations of kinases involved in transduction of growth and proliferation signals. However, in many AML cases the identity and function of pathogenetic mutations remains obscure. Recent genomic sequencing efforts in AML and in other malignancies have identified new classes of oncogenic disease alleles. One recently identified class of genes mutated in cancer is those coding for enzymes involved in citrate metabolism: cytosolic isocitrate dehydrogenase 1 (IDH1) and its mitochondrial homolog IDH2 (Mardis et al., 2009; Parsons et al., 2008; Yan et al., 2009). IDH1 and IDH2 lesions occur in ~70% of patients with lower grade (grade II-III) brain tumors such as astrocytomas, as well as in secondary glioblastomas derived from lower grade glial tumors (Parsons et al., 2008; Yan et al., 2009). IDH1 and IDH2 mutations were subsequently observed in myeloid malignancies including *de novo* and secondary AML (~15-30%), and pre-leukemic clonal malignancies including myelodysplasia and myeloproliferative neoplasms (~5% of chronic phase and ~20% of transformed cases) (Mardis et al., 2009; Tefferi et al., 2010; Ward et al., 2010). The mutational data in malignant gliomas and in myeloid malignancies suggest that IDH1/2 mutations can occur early in disease pathogenesis and may drive tumorigenesis.

The precise genetic context in which IDH1/2 mutations occur is not known, nor is the mechanism through which they contribute to the malignant phenotype. IDH1/2 mutations

are heterozygous, with tumors retaining one wild-type copy of the relevant IDH1 or IDH2 allele, suggesting that the mutations are selected for an enzymatic gain of function rather than a loss of function (Dang et al., 2009; Ward et al., 2010), and that retention of the wild-type allele may be required for normal cellular metabolism. IDH1 and IDH2 are $NADP^+$-dependent enzymes that normally catalyze the interconversion of isocitrate and alpha-ketoglutarate (αKG - also known as 2-oxoglutarate). The most common IDH1/2 mutations in AML and brain tumors, affecting R132 of IDH1 or R140 and R172 of IDH2, have the common feature of acquiring a neomorphic enzymatic activity catalyzing the NADPH-dependent reduction of αKG to R(-)-2-hydroxyglutarate (2HG) (Dang et al., 2009; Ward et al., 2012). Presumably it is the production of 2HG that provides a biological advantage that contributes to malignant transformation. As 2HG is a structural analogue of αKG, differing only in the substitution of the alpha-keto group on αKG for a hydroxyl group, it is plausible that generation of 2HG by mutant IDH1 and IDH2 might impair the function of enzymes that require αKG as a substrate.

Recent epigenetic studies of large AML patient cohorts have demonstrated that aberrant DNA methylation is a hallmark of AML (Figueroa et al., 2010b). Importantly, promoter methylation data can be used to classify AML in distinct clusters defined by specific patterns of methylation. Although a subset of DNA methylation signatures have been found to be associated with known genetic mutations, specific AML subsets were recognized solely based on their DNA methylation profiles (Figueroa et al., 2010b). It is not currently known whether there are somatic genetic events that define any of the novel epigenetic clusters in AML. The recent finding that glioblastomas with a methylator phenotype are associated with cytosolic IDH1 mutations suggested a potential causative

link between these features, although mutations of the mitochondrial IDH2 enzyme were not detected in this study and as such the relationship between IDH2 mutations and epigenetic state could not be assessed (Noushmehr et al., 2010). Interestingly, loss-of-function mutations of TET2, an αKG-dependent enzyme that converts 5-methylcytosine to 5-hydroxymethylcytosine (Tahiliani et al., 2009), were also identified in AML (Delhommeau et al., 2009).

We report that in a cohort of AML patients, IDH1/2 mutations and TET2 mutations showed remarkable mutually exclusivity. Consonant with the mutational data, IDH mutants inhibited the function of TET2 and induced global hypermethylation and increased hematopoietic stem cells marker, which is a characteristic feature of AML. Collectively the data suggest increased cellular 2HG levels induced by mutant IDH isoforms contribute to malignant transformation by interfering with the normal cycle of DNA methylation and demethylation through inhibiting αKG-dependent enzymes such as TET2.

Results

Mutations in *IDH1/2* are mutually exclusive with mutations in *TET2*

Specimens (385) from a total cohort of 398 patients with *de novo* AML younger than 60 years of age enrolled in the ECOG E1900 clinical trial (Fernandez et al., 2009) were subjected to DNA sequence analysis for AML-associated recurrent mutations. High-throughput resequencing of *IDH1* and *IDH2* revealed *IDH1* R132 mutations in 6.2% of patients and *IDH2* mutations in 8.6% of patients (6.3% R140Q and 2.3% R172K). Patients with mutations in *IDH1* or *IDH2* did not differ from *IDH1/2*-wild-type patients in terms of age, sex, or percentage of bone marrow blasts at diagnosis. No additional somatic *IDH1/2* mutations were found. All *IDH1* and *IDH2* mutations were heterozygous, consistent with retention of the wild-type allele as previously reported. Although mutations in *IDH1* and *IDH2* are thought to be mutually exclusive based on mutational studies in malignant gliomas (Yan et al., 2009), occasional rare AML patients have been reported with concurrent mutations in both *IDH1* and *IDH2* (Paschka et al., 2010). In this large cohort of patients with *de novo* AML, mutations in *IDH1* and *IDH2* were mutually exclusive.

TET2 is a Fe (II) and αKG-dependent enzyme known to display loss of function mutations in AML and other myeloid malignancies (Abdel-Wahab et al., 2009; Delhommeau et al., 2009). Recently all TET family members including TET2 were shown to catalyze the conversion of 5-methylcytosine to 5-hydroxymethylcytosine (5-OH-MeC) (Tahiliani et al., 2009). Although the physiological significance of 5-OH-MeC remains to be determined, it is likely to be the intermediate in the pathway that actively

demethylates 5-methylcytosine (Wu and Zhang, 2011). Importantly, expression of TET1 or TET2 in cellular systems results in a reduction in 5-methylcytosine levels (Ito et al., 2010). Unlike other DNA demethylases identified so far, the hydroxylation reaction does not involve any DNA damage, suggesting an important physiological function of TET2 in removing methylation marks.

We first examined the genetic status of *TET2* in AML samples wild-type or mutant for *IDH1/2*. As controls in analyzing for association with *TET2* mutations, we also examined the mutational status of 11 other genes known to be recurrently mutated in AML (including *PHF6*, *WT1*, *TP53*, *ASXL1*, *PTEN*, *RUNX1*, *KIT*, *NPM1*, *FLT3*, *CEBPA* and *RAS*) in this same cohort. There were 40 somatic *TET2* mutations identified in 28/385 patients (7.3% of the ECOG patient cohort). Although only 1 homozygous *TET2* mutation was observed, 11 of the 28 *TET2*-mutant patients had >1 *TET2* mutation, consistent with previous studies reporting biallelic *TET2* mutations. Of the 40 *TET2* mutations, 40% were insertions/deletions resulting in a frameshift mutation, 30% were nonsense mutations, and 30% were somatic missense mutations. AML patients with *TET2* mutations did not differ from *TET2* wild-type patients in terms of age, sex, cytogenetic risk, or percentage of bone marrow blasts at diagnosis. *TET2* mutant patients also did not differ from *TET2* wild-type AML patients in frequency of mutations in *FLT3*, *NPM1*, or *CEBPA*.

In contrast to the other genes analyzed, the relationship between *IDH1/2* and *TET2* mutations was striking in this AML cohort. Although *IDH1*, *IDH2*, and *TET2* mutations were each identified in a significant proportion of patients in our study, there was a statistically significant inverse correlation between *IDH1/2* and *TET2* mutations in AML

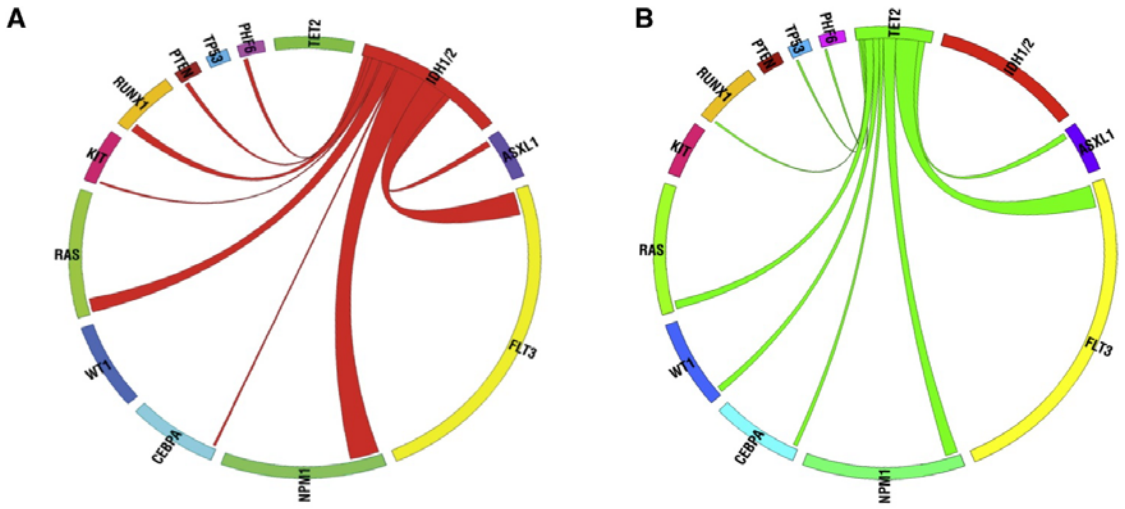

C

	TET2 Wildtype	*TET2* Mutant
IDH1/2 Wildtype	300	28
IDH1/2 Mutant	57	0

p value: 0.009 (left-tailed Fisher test)

Figure 2.1: *IDH1/2* mutations are mutually exclusive with mutations in *TET2* in *de novo* AML.

(A) Circos diagram revealing relative frequency and pairwise co-occurrences of mutations in *IDH1* and *IDH2* in *de novo* AML. (B) Circos diagram revealing relative frequency and pairwise co-occurrences of mutations in *TET2* in *de novo* AML. (C) Two-by-two table showing that mutations in *IDH1/2* and *TET2* were mutually exclusive in AML (Left-tailed Fisher *p*-value: 0.009).

(p=0.009, left-tailed Fisher's exact test). Specifically, we did not identify a single patient with concurrent mutations in *TET2* and in *IDH1* or *IDH2*; 0/57 *IDH1/2* mutant cases were *TET2* mutant versus 28/300 *IDH1/2* wild-type AML cases (Figures 2.1A-C). These data suggest that *TET2* and *IDH1/2* mutations form a novel mutational class in AML, and that *IDH1/2* mutations and *TET2* mutations have overlapping roles in AML pathogenesis.

IDH mutation inhibits the hydroxylation of 5-methylcytosine by TET2

TET2 has the classical features of an αKG –Fe(II) dioxygenase, and requires αKG in order to mediate 5-methylcystosine hydroxylation (Tahiliani et al., 2009). The five carbon dicarboxylic acids 2HG and αKG are chemically analogous. The substitution of the keto (oxo) group on αKG to hydroxyl group on 2HG could potentially interfere with Fe(II) binding and stabilization of the reaction intermediate. We therefore hypothesized that 2HG produced by mutant IDH might inhibit the hydroxylation of 5-methylcytosine by TET2. To test this hypothesis, we expressed FLAG-tagged TET2 in 293T cells. Consistent with previous findings (Ito et al., 2010; Tahiliani et al., 2009), cells expressing TET2 showed higher levels of 5-OH-MeC in the nucleus as detected by immunofluorescence staining with 5-OH-MeC specific antibody. Co-transfection of TET2 with IDH1 R132H, but not wild-type IDH1, reversed this increase in 5-OH-MeC (Figure 2.2A). To obtain a more quantitative assessment, we also performed flow cytometric analysis of 5-OH-MeC fluorescence intensity. Staining with an anti-FLAG antibody allowed us to discriminate between TET2-positive and TET2-negative populations; importantly the TET2-positive population showed a ~4-fold increase in the 5-OH-MeC fluorescence intensity. Co-transfection with R132H mutant IDH1 led to a ~40% decrease in the fluorescence intensity, while wild-type IDH1 had no significant

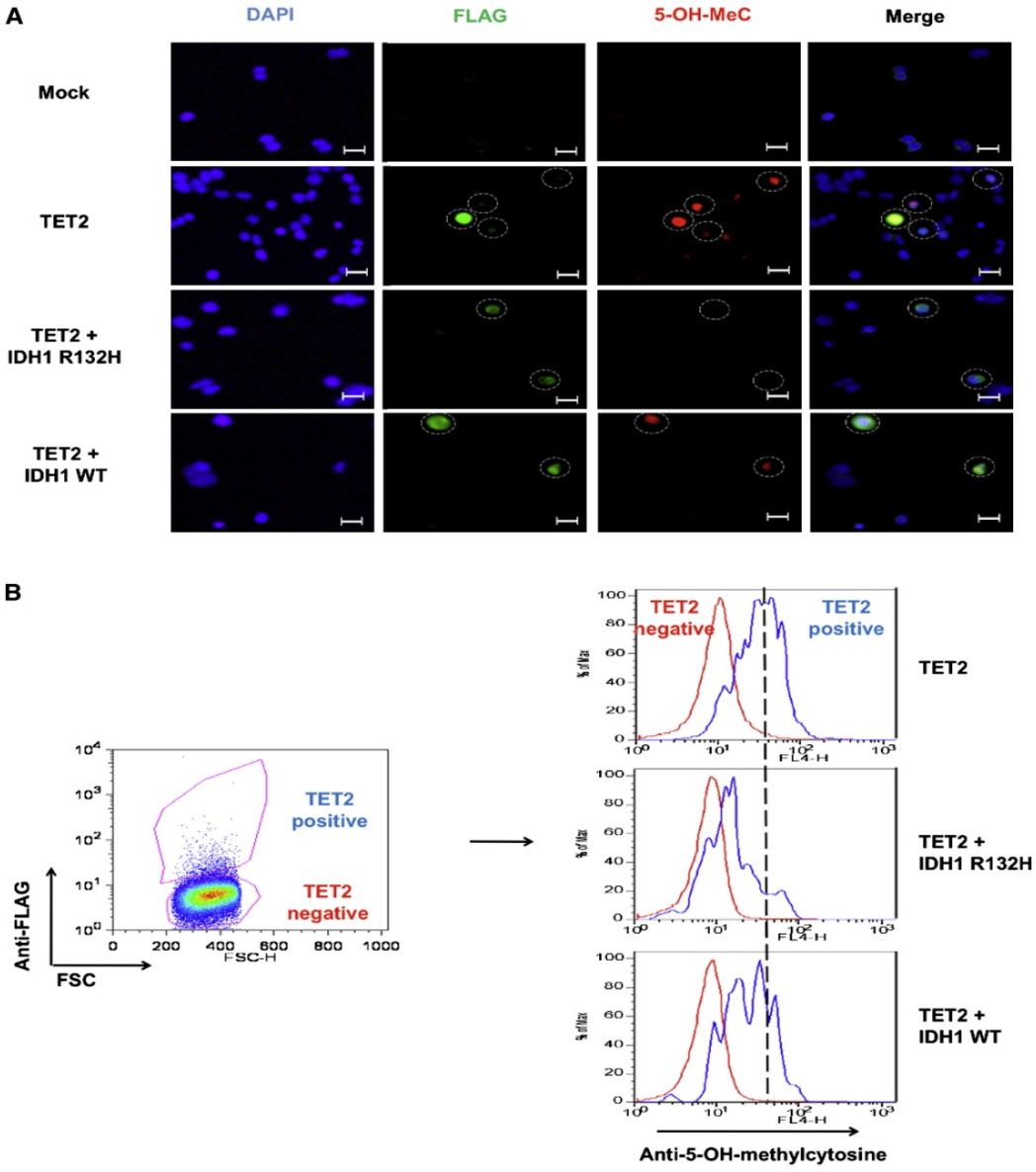

Figure 2.2: Mutant IDH1 expression inhibits hydroxylation of 5-methylcytosine by TET2.

(A) 293T cells were transiently transfected with FLAG-tagged TET2 in the absence or presence of wild-type or R132H mutant IDH1. Global levels of 5-methylcytosine hydroxylation were analyzed by immunofluorescence using antibody against 5-hydroxy-methylcytosine (5-OH-MeC). Representative images from mock-transfected, TET2-transfected, TET2 + IDH1 WT co-transfected, and TET2 + IDH1 R132H co-transfected cells are shown. (B) Transfected cells were analyzed by flow cytometry and gated as TET2 positive or negative by FLAG antibody. Representative gating is shown. Intensities of 5-OH-methylcytosine staining within the TET2 positive and negative populations are shown as histogram overlays. Data in (A) and (B) are representative of three independent experiments.

impact on 5-OH-MeC fluorescence intensity (Figure 2.2B). Together these data suggest that expression of mutant IDH is able to inhibit the hydroxylation of 5-methylcytosine by TET2.

Expression of 2HG-producing IDH mutant in cells induces a global decrease in 5-OH-MeC and increase in 5-methylcytosine

We next sought to determine whether expression of mutant IDH was sufficient to alter levels of 5-OH-MeC and 5-methylcytosine in myeloid cells. Wild-type or R172K mutant IDH2 were stably expressed in mouse myeloid progenitor 32D cells. Expression of wild-type and mutant IDH2 protein was confirmed by Western blot (Figure 2.3A). 2HG levels were measured by gas chromatography-mass spectrometry (GC-MS) and were only induced in cells stably expressing mutant IDH2 (Figure 2.3B). The levels of 5-OH-MeC and 5-methylcytosine were assessed by liquid chromatography-electrospray ionization tandem mass spectrometry (LC-ESI-MS/MS). Results showed that expression of R172K mutant IDH2 led to a significant decrease in global levels of 5-OH-MeC (Figure 2.3C). Consistent with the role of TET2 in DNA demethylation, we also observed an increase in global 5-methylcytosine levels (Figure 2.3D). These data support that 2HG-producing mutant IDH causes changes in DNA methylation and hydroxymethylation.

Mutant IDH and TET2 depletion both increase expression of stem cell markers

To investigate the biological significance of IDH1/2 mutations, the effects of stable expression of wild-type, R172K mutant or R140Q mutant IDH2 were examined in 32D myeloid cells. Expression of mutant IDH2, but not of wild-type IDH2 in 32D cells resulted in an average of ~40% increase in hematopoietic stem/progenitor cell marker C-

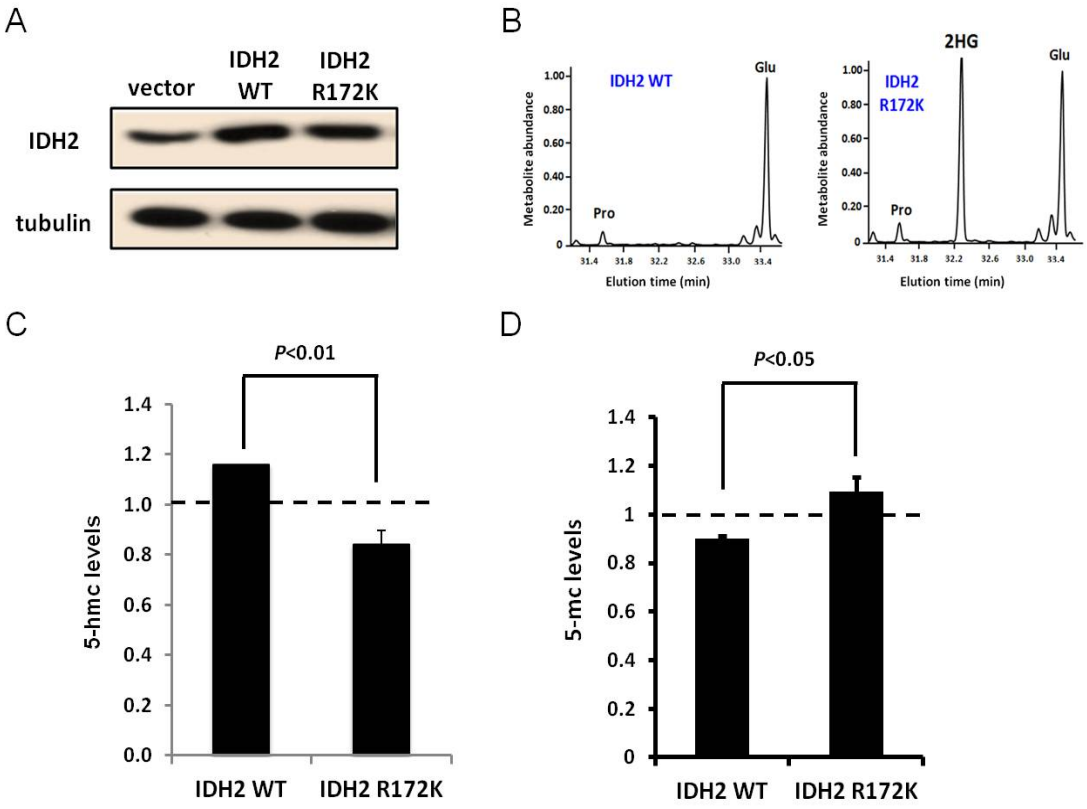

Figure 2.3: Expression of 2HG-producing IDH proteins alters global DNA methylation.

(A) 32D cells were transduced with empty retroviral vector or with wild-type or R172K mutant IDH2, selected in 2.5 μg/ml puromycin for 7 days, and then lysed to confirm stable expression of IDH2. Tubulin antibody was used as a control. (B) Cells were extracted for their intracellular metabolites which were then derivatized with MTBSTFA and analyzed by GC-MS. Shown are representative gas chromatographs from wild-type and mutant IDH2 expressing cells depicting the derivatized metabolites eluting between 31.3 and 33.5 min, including 4-oxoproline (4-oxo Pro), glutamate (Glu), and 2HG. Metabolite abundance refers to GC-MS signal intensity. (C) and (D) DNA was extracted from cells with stable wild-type or mutant IDH2 expression, and global 5-OH-MeC (C) or 5-methylcytosine (D) levels were measured by LC-ESI-MS/MS. Relative intensity of signals of three independent experiments was quantified. Error bars represent SD for triplicate experiments.

Kit expression (p=0.04; Figure 2.4A). Likewise, shRNA-mediated stable knockdown of Tet2 expression resulted in a significant increase in C-Kit expression (p=0.02; Figures 2.4B). These data suggest that expression of IDH mutant or reduction in Tet2 expression results in similar effects on enhancing stemness in hematopoietic cells.

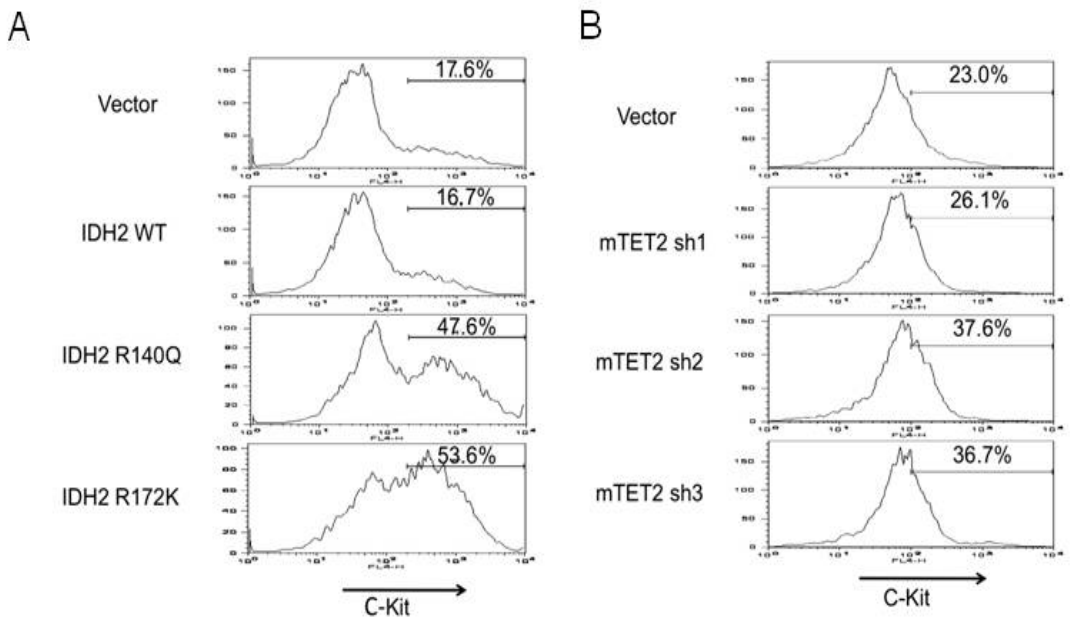

Figure 2.4: IDH2 mutant expression and TET2 knockdown in hematopoietic cells impairs differentiation.

(A) 32D cells retrovirally transduced with empty vector, IDH2 WT, IDH2 R140Q or IDH2 R172K were analyzed for C-Kit expression by flow cytometry. Intensities of fluorescence signals are depicted as histograms. (B) Three independent shRNAs against mouse TET2 were analyzed for C-Kit expression by flow cytometry. Intensities of fluorescence signals are depicted as histograms.

Discussion

We observed that *IDH1/2* and *TET2* mutations were mutually exclusive in a large, genetically annotated *de novo* AML cohort, suggesting that these lesions may be functionally redundant. TET2 is a member of a family of αKG-dependent enzymes that catalyze cytosine 5-hydroxymethylation and induce subsequent demethylation of DNA (Tahiliani et al., 2009). IDH1/2 mutations, which lead to elevated levels of 2HG, an αKG analogue, would be anticipated to inhibit the function of TET2 and to result in DNA hypermethylation. In support of this possibility we observed expression of IDH1/2 mutants induced an increase in global DNA hypermethylation, and inhibited TET2 induced cytosine 5-hydroxymethylation. These data suggest that TET2 and IDH1/2 mutations constitute a novel mutational class in AML which affects the epigenetic state; we would predict that additional mutations will be identified which will be classified into this novel "epigenetic regulator" mutational class in AML and in other malignancies.

The present data do not exclude the possibility that IDH1/2 mutant-mediated transformation is in part mediated by TET2 independent effects. Other families of enzymes that also require αKG for their catalytic activity, including Jumonji-C domain histone demethylases, could be affected by accumulation of 2HG in leukemic cells. Jumonji-C domain proteins can impair the spread of DNA methylation, alter the function of transcription factors and demethylate various chromatin marks including gene activation marks such as H3K4me3 and H3K36me3 (Tsukada et al., 2006) and gene repressive marks such as H3K9me3 (Yamane et al., 2006). It will therefore be important in subsequent studies to assess the effects of mutant IDH protein expression and 2HG accumulation on the function of other αKG-dependent enzymes expressed in

hematopoietic cells and on the chromatin state of normal and leukemic stem/progenitor cells. Moreover, whether other somatic lesions influence the IDH1/2 and TET2 mutant DNA methylation profiles awaits ongoing and future studies of AML genetic and epigenetic lesions.

Collectively, the data suggest a new paradigm whereby oncogenic alterations in core cellular metabolic pathways can lead to leukemic transformation by dysregulating the epigenetic machinery in hematopoietic progenitors. Additionally, the data support the notion that IDH1/2 mutants are a powerful leukemia driver. Since mutant IDH1/2 are associated with a neomorphic function not characteristic of the wild-type protein, targeted therapies that inhibit the neomorphic function of mutant IDH enzymes might reverse epigenetic patterning, promote myeloid differentiation, and improve outcomes in IDH1/2-mutant AML.

Chapter 3

IDH mutation impairs histone demethylation and results in a block to cell differentiation

Parts of this chapter have previously been published in: Lu C, Ward PS, Kapoor GS, Rohle D, Turcan S, Abdel-Wahab O, Edwards CR, Khanin R, Figueroa ME, Melnick A, Wellen KE, O'Rourke DM, Berger SL, Chan TA, Levine RL, Mellinghoff IK, Thompson CB. IDH mutation impairs histone demethylation and results in a block to cell differentiation. *Nature* 2012 483:474–78.

Summary

Recurrent mutations in isocitrate dehydrogenase 1 (IDH1) and IDH2 have been identified in gliomas, acute myeloid leukaemias (AML) and chondrosarcomas, and share a novel enzymatic property of producing 2-hydroxyglutarate (2HG) from α-ketoglutarate. 2HG-producing IDH mutants can prevent the histone demethylation that is required for lineage-specific progenitor cells to differentiate into terminally differentiated cells. In tumor samples from glioma patients, IDH mutations were associated with a distinct gene expression profile enriched for genes expressed in neural progenitor cells, and this was associated with increased histone methylation. To test whether the ability of IDH mutants to promote histone methylation contributes to a block in cell differentiation in non-transformed cells, the effect of neomorphic IDH mutants on adipocyte differentiation was tested *in vitro*. Introduction of either mutant IDH or cell-permeable 2HG was associated with repression of the inducible expression of lineage-specific differentiation genes and a block to differentiation. This correlated with a significant increase in repressive histone methylation marks without observable changes in promoter DNA methylation. Gliomas were found to have elevated levels of similar histone repressive marks. Stable transfection of a 2HG-producing mutant IDH into immortalized astrocytes resulted in progressive accumulation of histone methylation. Of the marks examined, increased H3K9 methylation reproducibly preceded a rise in DNA methylation as cells were passaged in culture. Furthermore, the 2HG-inhibitable H3K9 demethylase KDM4C was induced during adipocyte differentiation, and RNA-interference suppression of KDM4C was sufficient to block differentiation. Together these data demonstrate that 2HG can

inhibit histone demethylation and that inhibition of histone demethylation can be sufficient to block the differentiation of non-transformed cells.

Introduction

Isocitrate dehydrogenases (IDHs) are enzymes that interconvert isocitrate and α-ketoglutarate (αKG). Mutations in either cytosolic $NADP^+$-dependent IDH1 or mitochondrial $NADP^+$-dependent IDH2 were found in ~80% of grade II-III gliomas, ~20% of *de novo* adult acute myeloid leukemia (AML), ~56% of central and periosteal cartilaginous tumors, ~30% intrahepatic cholangiocarcinomas and ~20% angioimmunoblastic T-cell lymphoma (Amary et al., 2011; Borger et al., 2012; Cairns et al., 2012; Mardis et al., 2009; Parsons et al., 2008; Ward et al., 2010; Yan et al., 2009). In these types of malignancies, all mutations identified are heterozygous and resulted in amino acid substitution of R132 of IDH1 or R172 or R140 of IDH2. Studies on the structural and enzymatic activity of mutant IDHs revealed that the mono-allelic mutations give the enzymes a novel property: instead of generating αKG from isocitrate, mutant IDH converts αKG to 2-hydroxyglutarate (2HG) (Dang et al., 2009; Ward et al., 2012; Ward et al., 2010). Consistent with this finding, elevated 2HG levels were detected in tumor samples with IDH mutations (Dang et al., 2009; Ward et al., 2010). While a common biochemical feature of cancer-associated IDH mutations has been discovered, its cellular effects and functional role in tumorigenesis remain elusive.

In an effort to delineate the mechanism underlining IDH mutation-driven leukaemogenesis, we performed comprehensive profiling of known recurrent genetic mutations in specimens from a cohort of 385 AML patients. Strikingly, gain-of-function *IDH1/2* mutations were mutually exclusive with *TET2* loss-of-function mutations (Figueroa et al., 2010a). Because TET2 is an αKG-dependent enzyme that hydroxylates 5-methylcytosine and potentially involved in DNA demethylation (Ito et al., 2010;

Tahiliani et al., 2009), we hypothesized that 2HG, the structural analog of αKG, could act to inhibit TET2 and lead to abnormal DNA methylation. Indeed, expression of mutant IDH in cells impaired the conversion of 5-methylcytosine to 5-hydroxymethylcytosine by TET2 (Figueroa et al., 2010a). Moreover, *IDH1/2* and *TET2* mutations were associated with an overlapping DNA hypermethylation phenotype. Consistent with our observations in AML, IDH1 mutations in glioma were strongly associated with DNA hypermethylation (Noushmehr et al., 2010). However, mutations of TET family members have yet to be reported in brain tumors. Therefore it is possible that in glioma additional αKG-dependent enzymes mediate mutant IDH's effects on chromatin.

In addition to DNA methylation, post-translational modifications of histones are also important for chromatin organization and regulation of gene transcription. Particularly, histone lysine methylation is an integral part of the "histone code". Recently a family of histone lysine demethylases, known as Jumonji-C domain histone demethylases (JHDMs), was shown to actively demethylate histone lysine residues (Klose and Zhang, 2007; Tsukada et al., 2006; Yamane et al., 2006). Interestingly, JHDMs share a similar reaction mechanism with TET2 that requires αKG as co-factor. In this study, we demonstrated a direct role of 2HG in inhibiting JHDM, which leads to genome-wide increase in histone lysine methylation. Consistent with the role of histone methylation in regulating cell differentiation, we showed that mutant IDH arrested adipocyte differentiation. Gene expression microarray analysis of glioma samples revealed a signature for IDH1/2 mutation that is enriched for genes involved in differentiation. These findings underscored the importance of histone lysine methylation, in addition to DNA methylation, as the target of 2HG-producing IDH mutations.

Results

The fact that IDH mutations were identified in multiple cancers with disparate tissues of origin suggests that 2HG-producing mutant enzymes probably affect some fundamental cellular processes that facilitate tumor progression. To study the effects of IDH mutations, we collected and performed gene expression microarray analysis on tumor specimens from patients with grade II–III oligodendroglioma. Sequencing results revealed a high frequency of IDH mutations in oligodendroglioma (33 of the samples had the R132 *IDH1* mutation, 2 had the R172 *IDH2* mutation and 6 were wild type for *IDH1/2*). Supervised analysis found a statistically enriched gene signature in IDH-mutant samples (q value <10%, fold change >2; Figure 3.1A) that was independent of tumor grade and recurrence status and survived multiple testing corrections. Gene-ontology analysis identified the regulation of astrocyte and glial differentiation as the top two functional categories enriched in differentially expressed genes (Figure 3.1B). We previously reported that IDH mutation may promote leukaemogenesis by expanding the haematopoietic progenitor cell population and impairing haematopoietic differentiation (Figueroa et al., 2010a), and that such a phenotype could be attributed at least in part to mutant IDH-induced inhibition of TET2, an α-ketoglutarate (αKG)-dependent enzyme potentially involved in DNA demethylation (Ito et al., 2010; Tahiliani et al., 2009). Although DNA hypermethylation has been associated with IDH mutation in glioma samples (Noushmehr et al., 2010), no mutations in TET family members have been found in this disease. We explored the possibility that IDH mutation may affect additional αKG-dependent enzymes that contribute to the regulation of cell differentiation.

Histone lysine methylation is an integral part of the post-translational modifications of histone tails that are important for chromatin organization and regulation of gene transcription (Klose and Zhang, 2007). *In vitro* 2HG can competitively inhibit a family of αKG-dependent Jumonji-C domain histone demethylases (JHDMs) (Chowdhury et al., 2011; Xu et al., 2011). To determine whether IDH-associated changes in histone methylation could be observed in cells, we ectopically expressed wild-type or mutant IDH1 or IDH2 in 293T cells and found that mutant IDH1 or IDH2 led to a marked increase in histone methylation compared to the wild-type enzymes. Transient transfection of wild-type IDH2 can also lead to increased 2HG production. In all of the samples, the magnitude of increase in methylation correlated with the intracellular 2HG levels produced by IDH transfection (Figure 3.1C). To test whether histone lysine methylation was dysregulated in gliomas with IDH mutation, immunohistochemistry analysis of patient oligodendroglioma samples was performed for several well-characterized histone marks. Compared to tumors with wild-type IDH, there was a statistically significant increase in the repressive trimethylation of H3K9 (H3K9me3) and an increasing trend in trimethylation of H3K27 (H3K27me3) in tumors with IDH1 mutation (Figure 3.1D). No statistically significant difference was seen in trimethylation of H3K4 (H3K4me3), a mark associated with active transcription (data not shown). These data suggested that IDH mutations might preferentially affect the regulation of repressive histone methylation marks *in vivo*.

As IDH mutations were associated with glial tumors of the 'proneural' phenotype (Verhaak et al., 2010), we sought to determine whether the persistence of histone repressive marks promoted by mutant IDH was sufficient to block the differentiation of

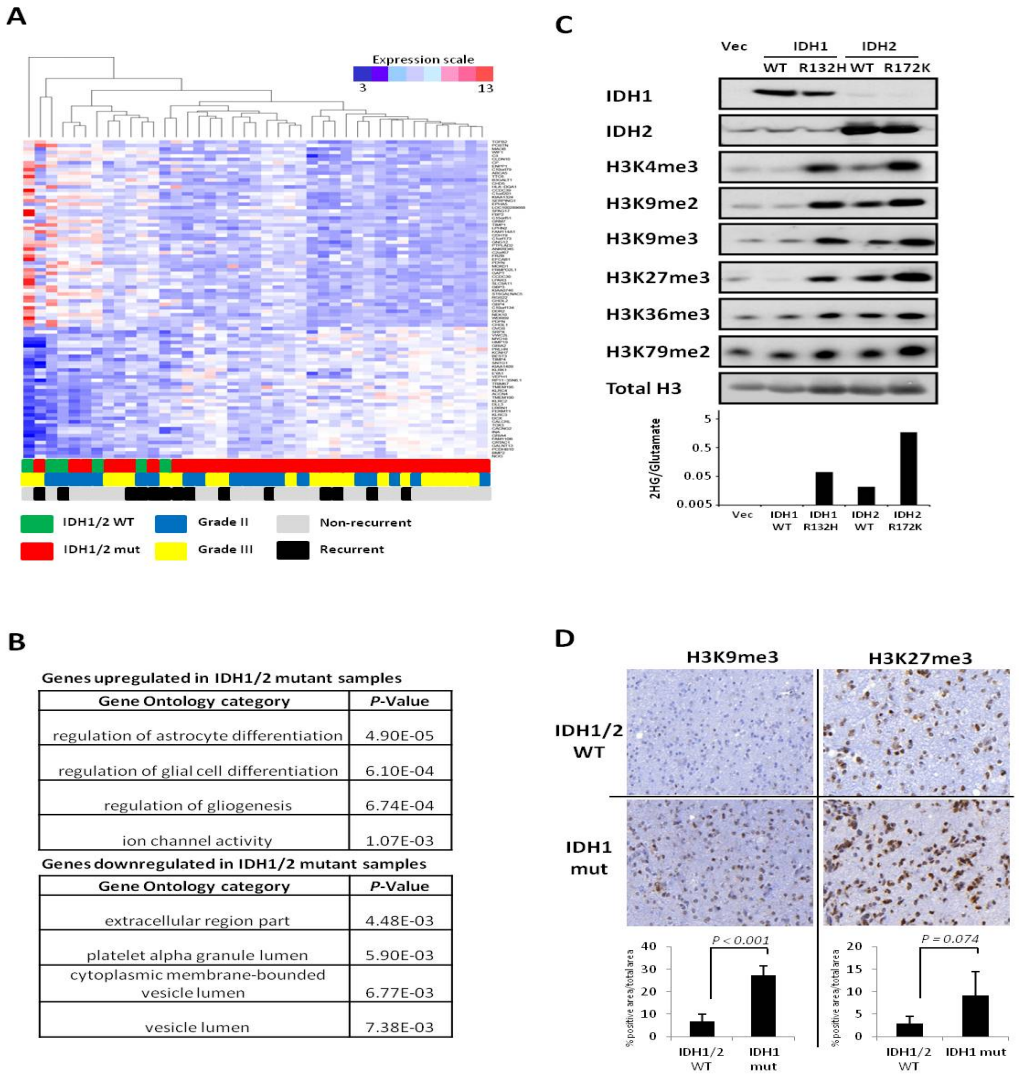

Figure 3.1: IDH mutations are associated with dysregulation of glial differentiation and global histone methylation.

(A) Heatmap representation of a two-dimensional hierarchical clustering of genes identified as differentially expressed between IDH1/2-mutant patient oligodendroglioma samples and IDH1/2-wild-type samples. Each row represents a gene and each column represents a specimen. IDH mutational status, tumor grade and recurrence of each sample are listed. (B) List of top four gene-ontology categories enriched in differentially expressed genes between IDH1/2-mutant vs. wild-type glioma samples. (C) 293T cells transfected with empty vector, wild-type or R132H mutant IDH1, or wild-type or R172K mutant IDH2 were lysed and assessed for expression levels of IDH1, IDH2 and histone lysine methylation marks by Western blotting with specific antibodies. Lower panel provides quantification of intracellular 2HG. (D) IHC staining with antibodies against H3K9me3 and H3K27me3 in IDH1/2 wild-type and IDH1 mutant oligodendroglioma samples. Image quantification was shown in lower panels.

non-transformed cells. Upon stimulation with a differentiation cocktail, immortalized murine 3T3-L1 cells undergo extensive chromatin remodelling, resulting in their maturation into adipocytes (MacDougald and Lane, 1995). 3T3-L1 cells transduced with R172K mutant IDH2 produced 2HG whereas cells transduced with either wild-type IDH2 or vector alone did not (Figure 3.2A). All three cell types were then induced to differentiate into adipocytes. After 7 days of differentiation induction, IDH mutant cells had visibly reduced lipid droplet accumulation compared to vector and IDH wild-type cells, as shown by Oil-Red-O staining (Figure 3.2B). To determine whether 2HG was sufficient to mediate the effect of mutant IDH on cell differentiation, we synthesized cell-permeable 1-octyl-d-2-hydroxyglutarate (octyl-2HG). Treatment of 3T3-L1 cells with octyl-2HG led to a dose-dependent inhibition of lipid accumulation (Figure 3.2C). Gene expression analysis showed that despite exposure to a well-standardized differentiation protocol, IDH mutant cells or cells treated with octyl-2HG exhibited a profound defect in the expression of transcription factors essential for executing adipogenesis (*Cebpa* and *Pparg*) and an adipocytic lineage-specific gene (*Adipoq*) (Figures 3.2D and 3.2E), suggesting that these cells failed to execute adipocyte differentiation.

Cells were harvested for a chromatin immunoprecipitation (ChIP) assay using antibodies against H3K9me3 and H3K27me3, before or after 4 days of differentiation induction. Quantitative polymerase chain reaction (PCR) with primers targeting promoters of *Cebpa* and *Adipoq* revealed that at day 4 there was a statistically significant increase in H3K9me3 and H3K27me3 at promoters of both genes in IDH mutant cells (Figure 3.3A). These repressive marks also showed a modest but significant increase at gene promoters

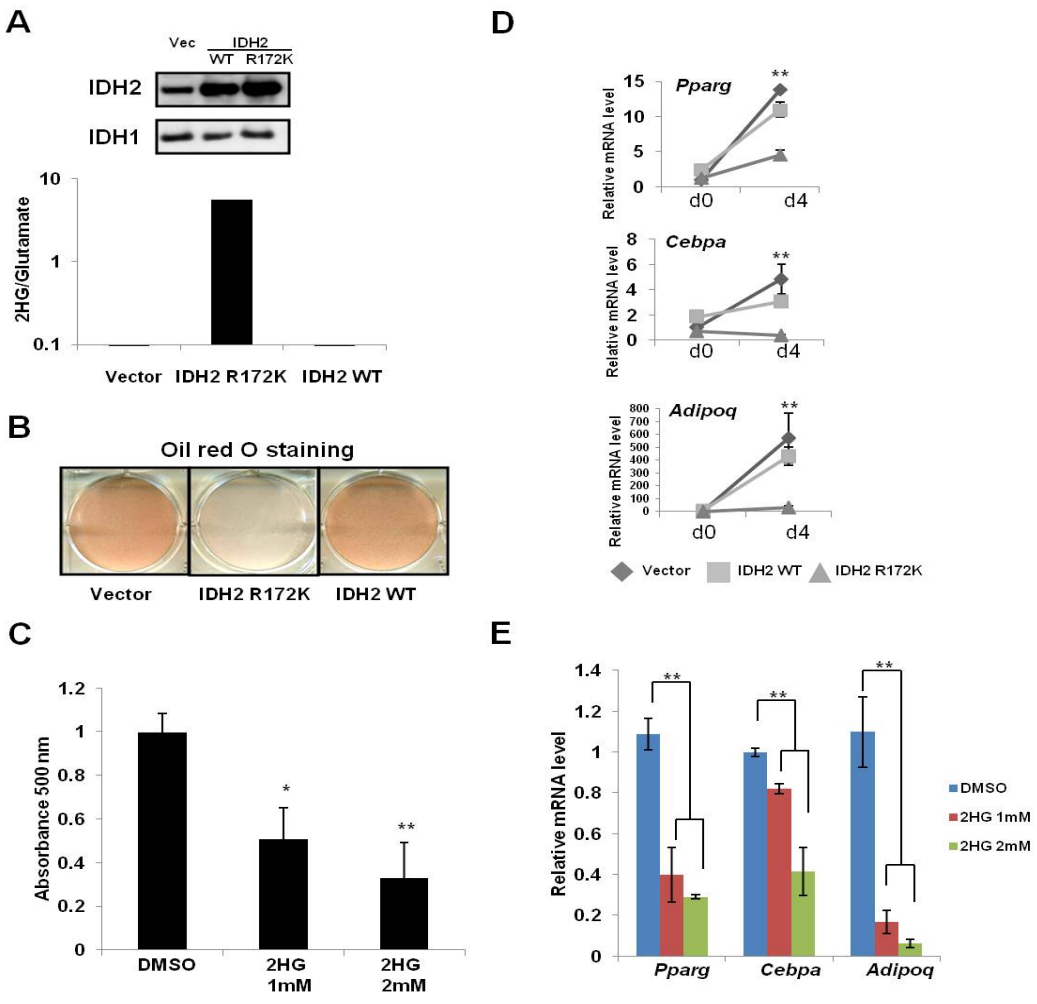

Figure 3.2: Differentiation arrest induced by mutant IDH or 2HG.

(A) 3T3-L1 cells stably expressing empty vector, wild-type, or R172K mutant IDH2 were lysed and assessed for expression levels of IDH2 or IDH1 by Western blotting. Cells were also extracted for intracellular metabolites which were then derivatized and analyzed by GC-MS. The quantification of 2HG signal intensity relative to the intrasample glutamate signal is shown. (B) Cells were induced to differentiate into mature adipocytes for 7 days. The accumulation of lipid droplets was assessed by Oil-red O staining. (C) 3T3-L1 cells were induced to differentiate for 7 days in the absence or presence of 1 mM or 2 mM octyl-2HG. Oil-red O staining was performed and quantified by measuring absorbance at 500 nm. (D) Vector, wild-type or R172K mutant IDH2 transduced 3T3-L1 cells were induced to differentiate for 4 days. RNA was extracted. Relative expression of genes was assessed by RT-qPCR. (E) 3T3-L1 cells were induced to differentiate for 4 days in the absence or presence of 1 mM or 2 mM octyl-2HG. RNA was extracted. Relative expression of genes was assessed by RT-qPCR. *, $p < 0.05$; **, $p < 0.01$; n.s., not significant.

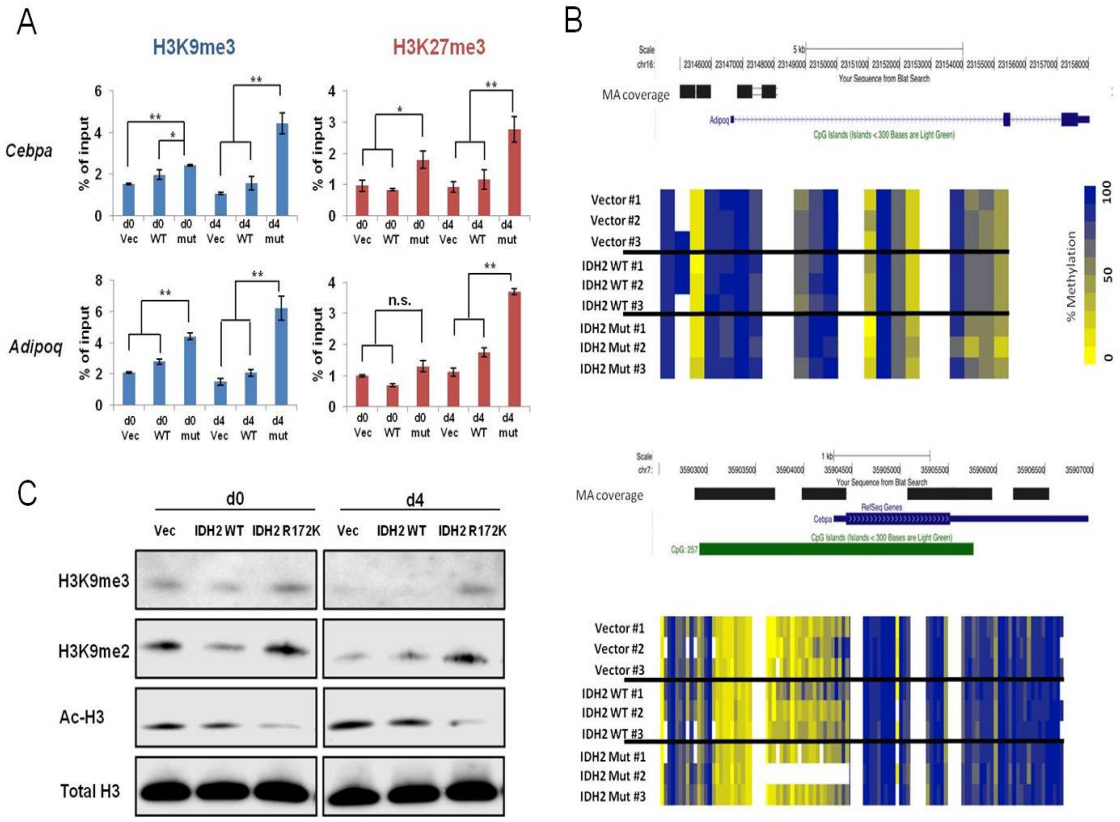

Figure 3.3: Differentiation arrest induced by mutant IDH is associated with increased global and promoter-specific H3K9 and H3K27 methylation.

(A) Vector, wild-type or R172K mutant IDH2 transduced 3T3-L1 cells were induced to differentiate. At d0 and d4, ChIP analysis was performed using antibodies against H3K9me3 and H3K27me3. Immunoprecipitated *Cebpa* and *Adipoq* promoter sequences were analyzed by qPCR and shown as percentage of input. Error bars indicate s.d. from triplicate wells. (B) 3T3-L1 cells stably expressing empty vector, wild-type, or R172K mutant IDH2 were induced to differentiate into mature adipocytes for 4 days. DNA was extracted from cells and bisulfite-converted. Promoter DNA methylation levels were assessed by MassARRAY (Sequenom). MassARRAY coverage for each promoter was indicated. Percentage of methylation was shown for triplicate samples from each condition. (C) Vector, wild-type or R172K mutant IDH2 transduced 3T3-L1 cells were induced to differentiate for 4 days. At days 0 and 4 (d0 and d4), histones were acid-extracted and levels of H3K9me3, H3K9me2 and acetyl-H3 were assessed by Western blotting with specific antibodies. Total H3 was used as loading control. *, $p < 0.05$; **, $p < 0.01$; n.s., not significant.

before differentiation induction. In contrast, quantitative assessment of DNA methylation at promoters of *Cebpa* and *Adipoq* by MassARRAY failed to reveal any significant difference between IDH wild-type and mutant cells (Figure 3.3B). In addition to gene-specific changes, we detected a global increase in H3K9 methylation and a reciprocal decrease in H3 acetylation (Figure 3.3C).

To determine whether IDH mutation was sufficient to induce enhanced repressive histone methylation in central nervous system (CNS)-derived cells and whether it was associated with altered neural gene expression, we retrovirally transduced immortalized normal humanastrocytes (NHAs) with either wild-type or R132H mutant IDH1. Compared to parental cells, late-passage cells expressing mutant IDH exhibited elevated levels of a variety of histone methylation marks (Figure 3.4A), and this correlated with an enhanced expression of the neural marker nestin (Figure 3.4B). Since IDH mutations have been associated with CpG-island hypermethylation and histone repressive marks can promote DNA methylation and vice versa, we studied the temporal relationship of histone and DNA methylation in IDH-expressing astrocytes (Figures 3.4C-3.4E). The first observable change of the histone marks we examined was H3K9me3. H3K9me3 levels were significantly elevated by passage 12 after cells were infected with mutant IDH. Changes in other histone methylation marks were either delayed and of lower magnitude (H3K27me3 and H3K79me2) or were not observed (H3K4me3). Increases in DNA methylation were never observed before passage 17 and the difference in DNA methylation reached statistical significance only at passage 22.

To test whether the IDH1 R132H mutation could interfere with neural differentiation in the absence of prolonged adaptation in culture, primary neurosphere cultures established

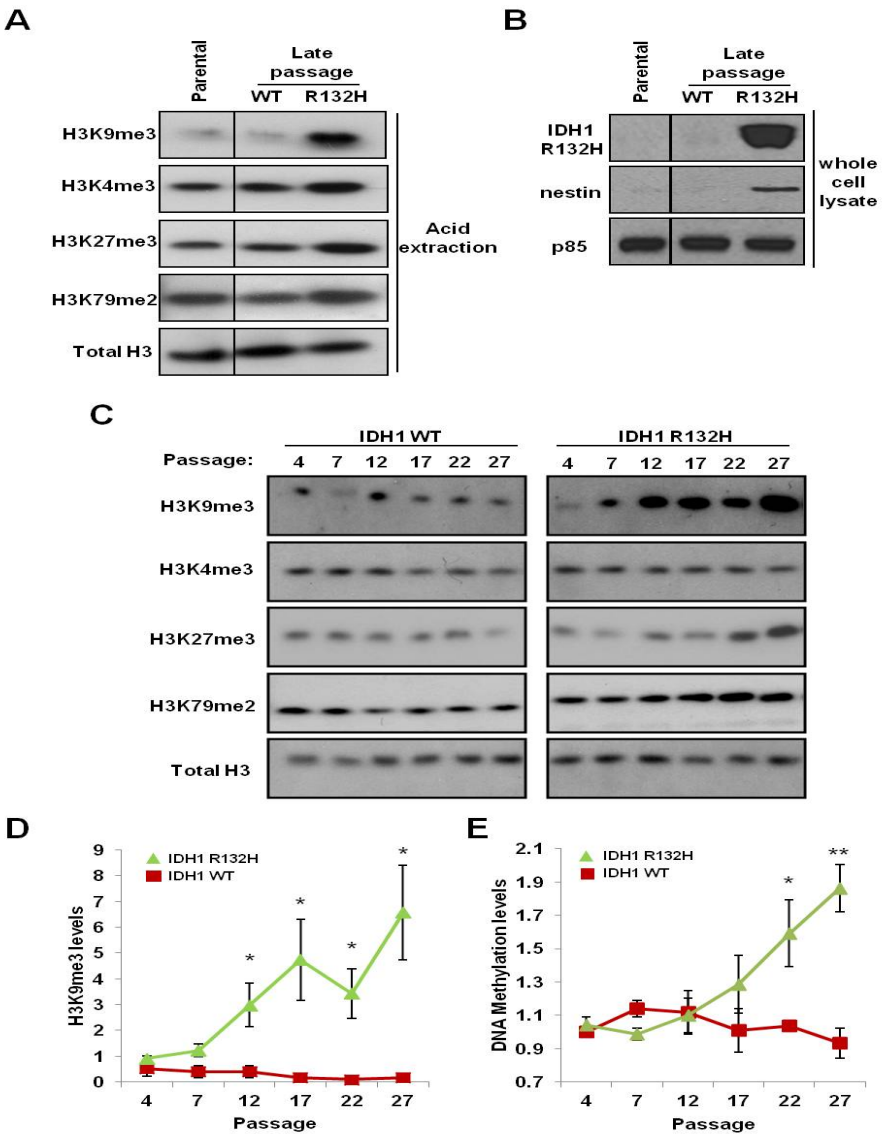

Figure 3.4: IDH mutation induces histone methylation increase in CNS-derived cells.

(A) Histones from parental NHA cells or cells transduced with wild-type or R132H mutant IDH were acid-extracted at late (>40) passages. Histone lysine methylation levels were assessed by Western blotting with specific antibodies. (B) Parental, IDH1 wild-type and R132H mutant NHA cells at late passages were lysed and assessed for expression levels of nestin by Western blotting. (C) Histones from NHA cells transduced with wild-type or R132H mutant IDH were acid-extracted at different time points as cells were passaged in culture. Histone lysine methylation levels were assessed by Western blotting with specific antibodies. (D) Western blot band intensities of H3K9me3 were quantified using Image J. (E) Total CpG methylation of IDH1 wild-type and R132H mutant NHA cells at various passages was measured by FACS using 5-methylcytosine-specific antibody and shown as normalized mean fluorescence intensity.

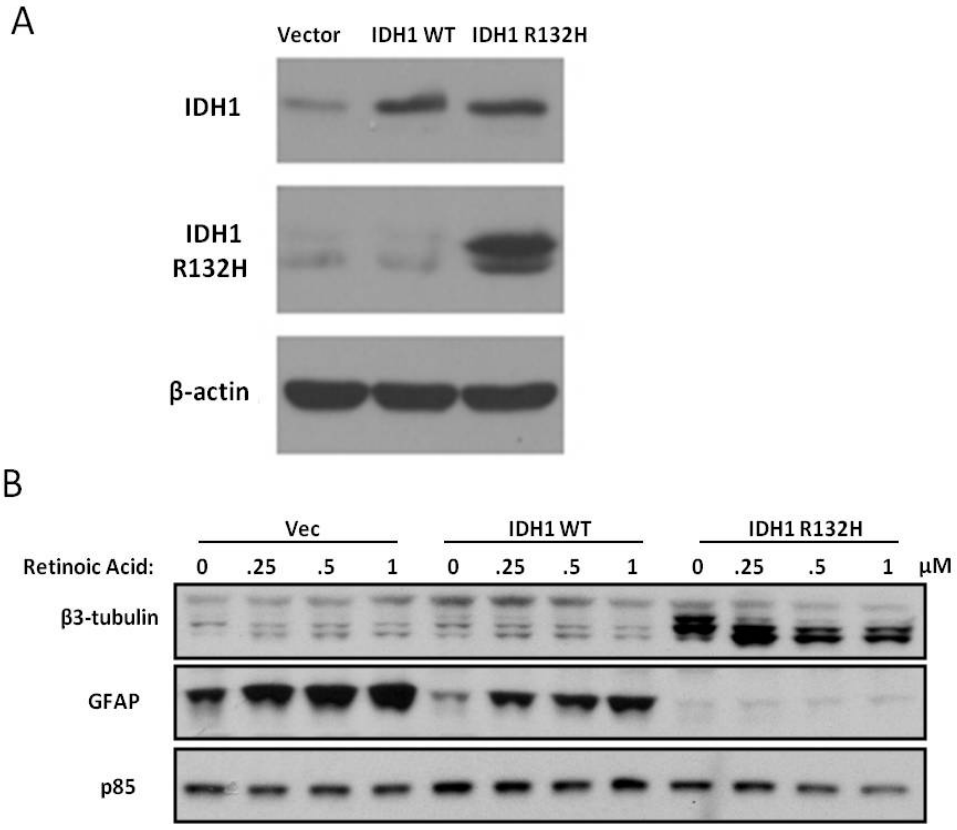

Figure 3.5: IDH mutation can alter cell lineage gene expression.

(A) Primary neurosphere cultures established from the brains of p16/p19$^{-/-}$ mice were retrovirally transduced with empty vector, wild-type or R132H mutant IDH1. Levels of protein expression of wild-type IDH1 or mutant IDH1 were analyzed by Western blotting with specific antibodies. (B) Neurosphere cultures established from the subventricular zone of brains of p16/p19$^{-/-}$ mice were infected with a retroviral construct containing IDH1 R132H mutant, wild-type IDH1 or the vector alone and induced to differentiate. GFAP and β3-tubulin expression levels were assessed by Western blotting. p85 was used as loading control.

from the brains of p16/p19$^{-/-}$ mice were infected with a retroviral construct containing IDH1 R132H mutant, wild-type IDH1 or the vector alone (Figure 3.5A). After infection the cells were re-plated under conditions that promote astrocyte differentiation and induced to differentiate further by treatment with retinoic acid without further passaging. IDH mutant cells failed to induce expression of the astrocytic marker GFAP and exhibited expression of the neural marker β3-tubulin (Figure 3.5B). When the differentiation conditions were supplemented with retinoic acid, enhanced expression of the astrocytic marker GFAP was observed in IDH wild-type and vector cells but GFAP expression remained repressed in IDH mutant cells.

The enhancement of H3K9 methylation in mutant IDH-expressing cells from multiple tissues of origin led us to investigate whether this H3K9 methylation might be sufficient to block the ability of non-transformed cells to execute differentiation. Support for this hypothesis came with the discovery that KDM4C (also known as JMJD2C), an H3K9-specific JHDM, was induced in 3T3-L1 cells during differentiation (Figure 3.6A). An *in vitro* histone demethylase assay with recombinant human GST-tagged KDM4C confirmed that KDM4C effectively removed H3K9me2 and H3K9me3 in the presence of αKG. Importantly, the demethylation reaction was inhibited by 2HG in a dose-dependent manner (Figures 3.6B and 3.6C). Given the similarities between 2HG and αKG, the inhibition of KDM4C by 2HG would be predicted to be competitive. Consistently, increasing the concentration of αKG in the reaction mixture reversed the inhibition of H3K9 demethylation by 2HG (Figure 3.6D).

Finally, to test the possibility that H3K9 demethylation is a required component of adipocyte differentiation, we examined whether blocking the induction of KDM4C was

sufficient to impair the differentiation of 3T3-L1 cells. Treatment with short interfering RNA (siRNA) against KDM4C reduced its expression and enhanced H3K9me3 in 3T3-L1 cells (Figures 3.7). After differentiation induction, cells treated with KDM4C siRNA exhibited reduced ability to differentiate into adipocytes (Figures 3.7). Thus the inability to erase repressive H3K9 methylation can be sufficient to impair the differentiation of non-transformed cells.

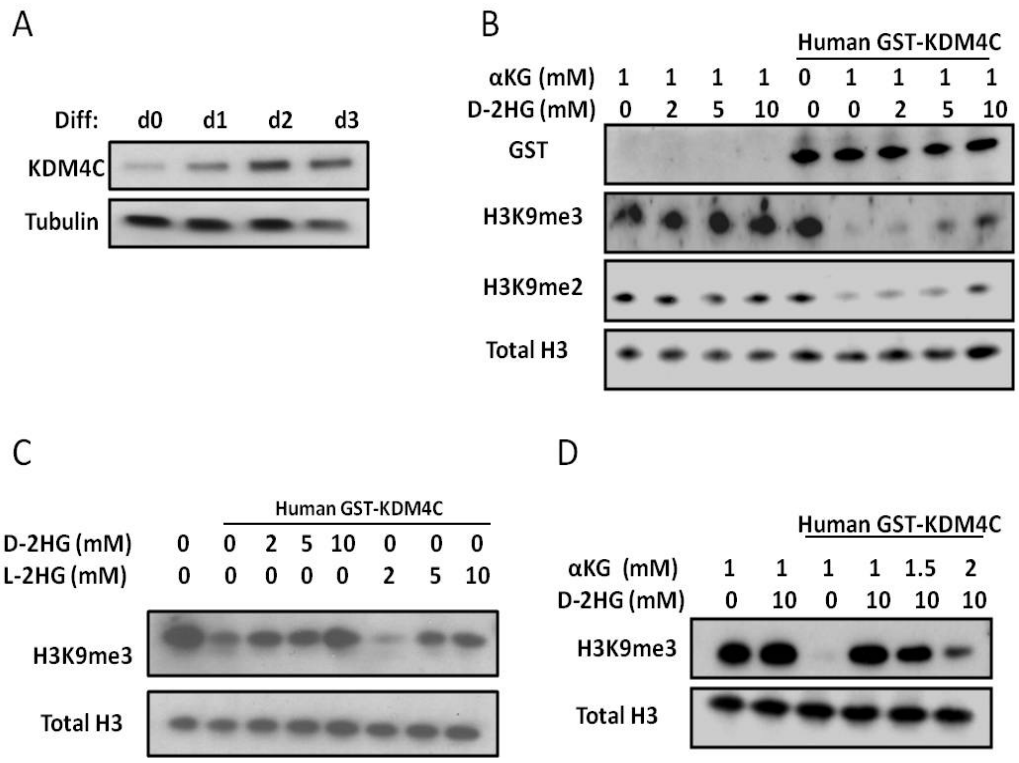

Figure 3.6: 2HG inhibits H3K9 demethylase KDM4C.

(A) 3T3-L1 cells were induced to differentiate for 3 days. Before (d0) and each day after differentiation induction, cells were lysed and KDM4C protein levels were assessed by Western blotting with specific antibody. (B) Bulk histones were incubated with purified GST-tagged human KDM4C in the reaction mix with 1 mM αKG and increasing concentrations of D-2HG. Levels of GST-tag, H3K9me3 and H3K9me2 were assessed by Western blotting with specific antibodies. (C) Bulk histones were incubated with purified GST-tagged human KDM4C in the reaction mix with 2, 5 or 10 mM D-2HG or L-2HG. Levels of H3K9me3 were assessed by Western blotting with specific antibody. (D) Bulk histones were incubated with purified GST-tagged human KDM4C in the reaction mix. 10 mM D-2HG was added to inhibit the demethylation reaction in the presence of increasing concentrations of αKG. Levels of H3K9me3 were assessed by Western blotting with specific antibody.

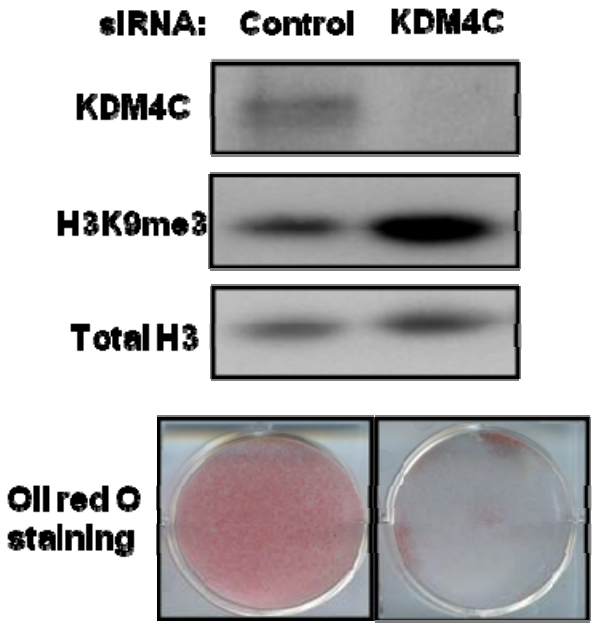

Figure 3.7: KDM4C is required for cell differentiation.

3T3-L1 cells were transfected with control siRNA or siRNA specific for KDM4C. After three days, cells were lysed and assessed for expression levels of KDM4C and H3K9me3 by Western blotting with specific antibodies. Cells from the same treatment were induced to differentiate for 7 days. The accumulation of lipid droplets was assessed by Oil-red O staining. Wells from a representative experiment from a total of 3 independent experiments are shown.

Discussion

Biochemical studies suggest that 2HG is a universal inhibitor of JHDM family members (Chowdhury et al., 2011; Xu et al., 2011); therefore it was interesting to observe that H3K9 demethylation seemed to be more sensitive to mutant IDH-induced suppression than at least some other histone methylation marks. This may be because H3K9 demethylases are more sensitive to inhibition by 2HG in comparison to other JHDM family members. Alternatively, H3K9 methylation is a histone mark that positively correlates with DNA methylation and participates in repressive heterochromatin formation associated with HP1 recruitment. H3K9 methylation is also mutually exclusive with H3K9 acetylation, a mark that positively correlates with increased gene expression and the promotion of H3K4 methylation at promoters (Latham and Dent, 2007). The fact that H3K27me3 can also significantly increase in response to IDH mutation suggests that there is a potential crosstalk between H3K9 methylation and Trithorax and Polycomb group proteins that regulate H3K4 and H3K27 methylation, respectively. In addition, given the delayed kinetics of other alterations in histone marks following introduction of mutant IDH, some of these changes may result from a mutant IDH-induced block in differentiation rather than direct inhibition of the relevant demethylases. It should be noted that KDM4C is not the only H3K9 demethylase and the fact that H3K9 methylation is increased in mutant IDH-infected fibroblasts prior to the induction of adipocytic differentiation suggests that 2HG is affecting additional H3K9 demethylases which have been shown to share a structurally similar binding pocket but can exhibit tissue-and development-specific variations in their expression (Ng et al., 2007). Future investigation

of the sensitivity to 2HG inhibition among JHDM family members and/or cellular feedback mechanisms activated after defective histone demethylation will be needed.

In addition to the data presented here, evidence is mounting for a direct role of histone methylation in stem cell maintenance, differentiation and tumorigenesis. For example, the *MLL* gene, which encodes a H3K4 methyltransferase, is involved in chromosomal rearrangement in ~80% of infant leukemia and 5-10% of adult AML (Krivtsov and Armstrong, 2007). KDM3B (also known as JMJD1B) is an H3K9 demethylase which is located at chromosome 5q31, a region frequently deleted in AML and myelodysplastic syndrome (Hu et al., 2001). More recently, systematic mutational screens of the coding genome identified inactivating mutations of KDM6A (H3K27 demethylase, also known as UTX) in a large array of cancers (van Haaften et al., 2009). A direct role of histone methylation in stem cell maintenance and differentiation has also been shown. For example, loss of KMT1E (also known as SETDB1), a H3K9 methyltransferase, resulted in impaired stem cell renewal (Bilodeau et al., 2009). Recently, KMT1E was found to be recurrently amplified in melanoma and accelerated melanoma onset after BRAF mutation (Ceol et al., 2011). The present data suggest that 2HG-producing IDH mutations represent an additional mechanism to impair the function of histone demethylases and thus block cellular differentiation.

Chapter 4

Differentiation blockade, resistance to contact inhibition and tumorigenesis by mutant IDH involves DNA hypermethylation

Summary

Frequent mutations of the metabolic enzymes isocitrate dehydrogenase 1 (IDH1) and IDH2 are found in multiple types of cancer. The mutations result in the accumulation of 2HG, a putative "oncometabolite" which is believed to mediate the oncogenic potential of mutant IDH. However, it is unclear whether mutant IDH is sufficient for tumorigenesis *in vivo* and the role of 2HG in the transformation process. Furthermore, despite strong evidence linking IDH mutation to DNA and histone hypermethylation, it remains to be shown that epigenetic misregulation contribute to the malignant phenotype caused by mutant IDH. Here we report that in a non-transformed murine mesenchymal multipotent cell line, expression of an IDH mutant impaired mesenchymal differentiation, induced loss of contact inhibition and generated highly mitotic mesenchymal tumors in xenograft study. DNA methylation profiling at base-resolution revealed a profound genome-wide CpG hypermethylation in IDH mutant cells which is enriched for genes involved in cell-cell contact. Our data suggest that epigenetic abnormality and the resultant aberrant gene expression represent a critical step in the initiation and progression of tumors with IDH mutation.

Introduction

Since the original observation by the German biochemist Otto Warburg that cancer cells utilize glucose in a fundamentally different way from normal cells (Warburg, 1956), the recent resurgence in cancer metabolism research led to the increasing appreciation that metabolic reprogramming is a hallmark of cancer (Vander Heiden et al., 2009; Ward and Thompson, 2012). However, it remains controversial whether metabolism rewiring observed in cancer plays a significant role in driving cancer development. A strong argument in support of this hypothesis is the recent identification of cancer-associated germline and somatic alterations of genes encoding for metabolic enzymes (Mullarky et al., 2011; Oermann et al., 2012), including prevalent mutations in isocitrate dehydrogenase 1 (IDH1) and IDH2.

Cytosolic IDH1 and mitochondrial IDH2 are $NADP^+$ -dependent enzymes that metabolize isocitrate to αKG. Frequent somatic mutations of IDH1 and IDH2 were identified in intermediate-grade gliomas (Yan et al., 2009), adult *de novo* acute myeloid leukemias (AMLs) (Mardis et al., 2009; Ward et al., 2010) and subsets of chondrosarcomas, lymphomas and cholangiocarcinomas (Amary et al., 2011; Borger et al., 2012; Cairns et al., 2012). The fact that mutations observed in IDH1 and IDH2 are always heterozygous point mutations affecting only a few residues suggests that they are unlikely loss of function. Indeed, metabolomic and biochemical analysis revealed that mutant IDHs gain a neomorphic activity of producing 2-hydroxyglutarate (2HG) from αKG (Dang et al., 2009; Ward et al., 2010). 2HG is normally present at very low levels in cells and as high as 100-fold increase in 2HG was observed in patient samples with IDH

mutation. It is believed that IDH mutations promote tumorigenesis through accumulating the putative "oncometabolite" 2HG.

At the molecular level, mounting evidence implicate a link between IDH mutation and epigenetic dysregulation, particularly DNA hypermethylation. In multiple malignancies, IDH mutations are tightly associated with a CpG island methylator phenotype (CIMP) in patient samples (Figueroa et al., 2010a; Noushmehr et al., 2010; Pansuriya et al., 2011; Wang et al., 2012), and expression of an IDH mutant in cell lines is sufficient to cause DNA hypermethylation (Figueroa et al., 2010a; Turcan et al., 2012). Mechanistically, mutant IDH was shown to impair activities of αKG-dependent chromatin modifying enzymes by producing 2HG as a competitive inhibitor. These include TET family enzymes which converts 5-methylcytosine (5mC) to 5-hydroxymethylcytosine (5hmC), a novel epigenetic mark potentially involved in DNA demethylation (Figueroa et al., 2010a); as well as Jumonji-C histone demethylases (Chowdhury et al., 2011; Lu et al., 2012). Importantly, genetic profiling of AML samples revealed a mutual exclusivity between IDH mutations and TET2 loss of function mutations, providing strong genetic evidence that IDH mutation may support tumorigenesis through modulating αKG-dependent chromatin modifier and the resultant hypermethylation of DNA and histone.

Despite the advance in understanding the molecular mechanism, it is yet to be shown whether mutant IDH is sufficient for tumorigenesis. Here we report that in a non-transformed murine mesenchymal progenitor cell line, IDH mutation leads to impaired mesenchymal lineage differentiation and loss of contact inhibition. Importantly, mutant IDH cells form highly mitotic tumors in mouse xenograft study. DNA methylation sequencing at base-pair resolution showed that IDH mutant cells display genome-wide

DNA hypermethylation, including key genes involved in cell adhesion. Collectively our data suggest that increased DNA methylation represents a critical step in the transformation by mutant IDH.

Results

IDH mutation inhibits mesenchymal lineage differentiation

We have previously reported that IDH mutation could block the adipocyte differentiation from non-transformed mouse 3T3-L1 fibroblasts (Lu et al., 2012). To determine the generality of these findings, we retrovirally transduced C3H10T1/2 (10T) cells with vectors containing either wild-type or R172K mutant IDH2. 10T cells were originally isolated from C3H mouse embryo. They were sensitive to confluence-induced proliferation arrest and showed no tumorigenicity in xenograft study (Reznikoff et al., 1973). Subsequently, 10T cells were demonstrated to be multipotent with the ability to differentiate into several mesenchymal lineages, including adipocytes, myoblasts and chondrocytes (Taylor and Jones, 1979). Notably, IDH mutations are found at high frequencies in chondrocytic sarcomas (Amary et al., 2011). 10T cells expressing R172K mutant IDH2 but not empty vector or wild-type (WT) IDH2 showed significant increase in 2HG levels (Figures 4.1A and 4.1B).

Consistent with previous findings, upon adipogenesis induction, IDH2 mutant cells showed a profound impairment in adipocyte differentiation with a lack of lipid droplets accumulation and absence of adipocyte-specific gene expression (*Adipoq* and *Fabp4*) compared to vector and WT IDH2 cells (Figure 4.1C). Similarly, when cells were subjected to conditions that promote chondrogenesis, morphological conversion from fibroblast-like to rounded shapes resembling mature chondrocytes and expression of chondrocyte-specific markers *Acan* and *Col2a1* were only observed in vector and WT IDH2 cells but not IDH2 mutant cells (Figure 4.1D). Furthermore, while vector and WT

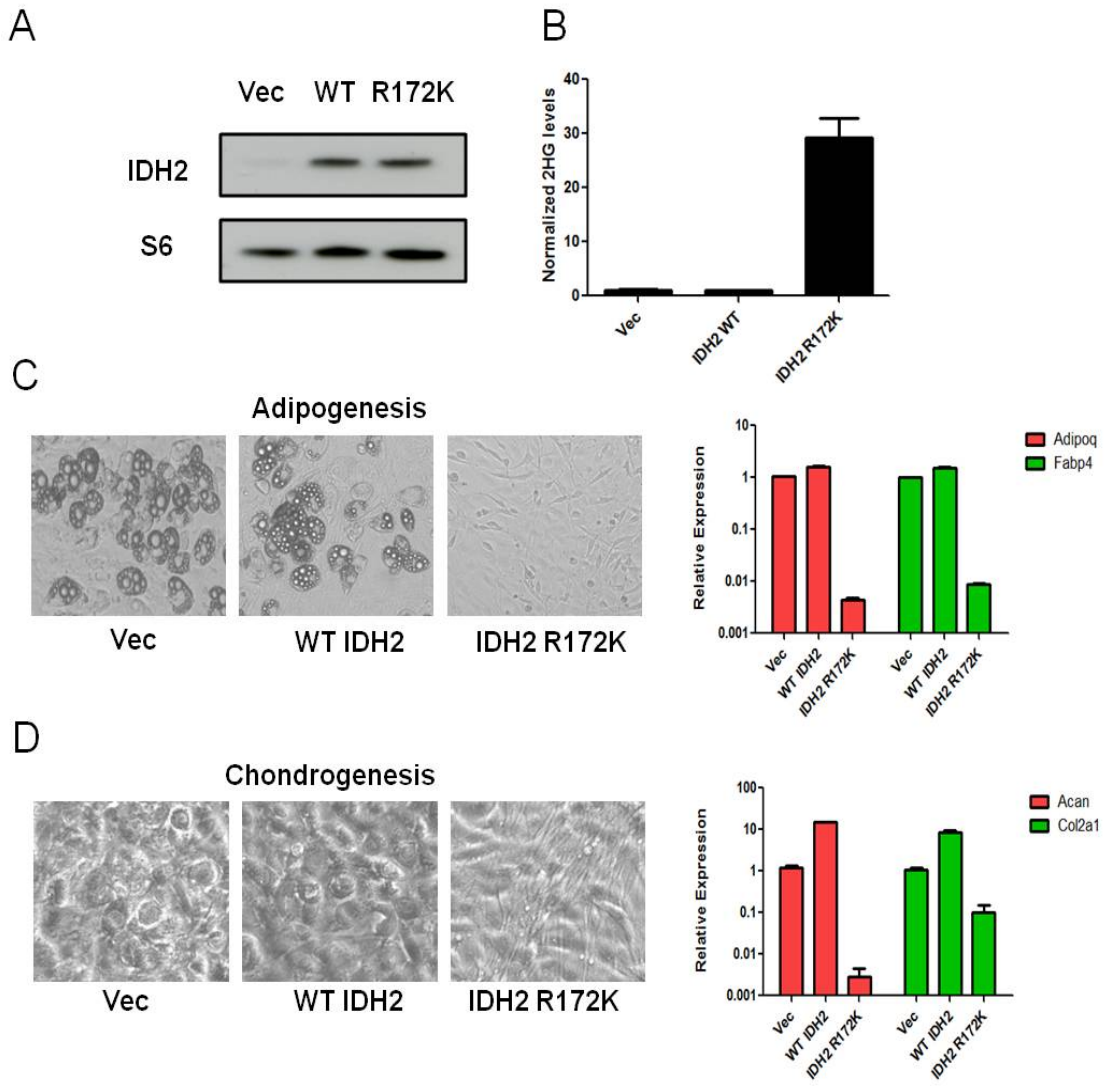

Figure 4.1: IDH mutation inhibits mesenchymal lineage differentiation.

(A) 10T cells were retrovirally transduced with empty vector or vectors containing either WT or R172K mutant IDH2. After puromycin selection, levels of IDH2 protein were assessed by Western blot. (B) Levels of 2HG measured by GC-MS in 10T cells expressing vector, WT or mutant IDH2. (C) Vector, WT or mutant IDH2 cells were treated with adipogenesis cocktail. Microscopic images of cell morphology were recorded 7 days after differentiation. mRNA expression of *Adipoq* and *Fabp4* was measured by Q-RTPCR. (D) Vector, WT or mutant IDH2 cells were treated with chondrogenesis cocktail. Microscopic images of cell morphology were recorded 10 days after differentiation. mRNA expression of *Acan* and *Col2a1* was measured by Q-RTPCR.

IDH2 cells became growth arrested after the induction of adipocyte or chondrocyte differentiation, IDH2 mutant cells continued to proliferate (Figure 4.2A) and maintained high levels of cyclin D1 (Figure 4.2B). Taken together these data suggest that differentiation blockade by IDH mutation is a common feature shared by multiple mesenchymal lineages.

IDH mutant cells escape contact inhibition and generate tumors *in vivo*

The differentiation experiments described above require cells to be seeded at confluence before induction. Therefore the observations that IDH mutant cells were able to continue proliferation at post-confluence prompted us to determine whether these cells have become insensitive to contact inhibition. When cultured in normal growth medium, vector, WT IDH2 or IDH2 mutant cells showed no difference in proliferation rate at sparse (day 0 – day 2, Figure 4.3A). However, while vector and WT IDH2 cells stopped proliferation after reaching confluence (day 4 – day 6), the accumulation of IDH2 mutant cells continued even after confluency was achieved. Cell cycle analysis showed that IDH2 mutant cells had a higher percentage of cell population in G2 and S phase at post-confluence (Figure 4.3B). Moreover, the induction of cell cycle inhibitor p27 and the decrease in levels of cyclin D1 after contact inhibition were less pronounced in IDH2 mutant cells (Figure 4.3C).

IDH2 mutant cells underwent cell cycle arrest normally after serum deprivation (Figure 4.3D), suggesting that their escape from contact inhibition is unlikely due to defects in cell cycle regulation. The cadherins are critical components of cell-cell adhesion and have been proposed to be the main upstream mediator of contact inhibition

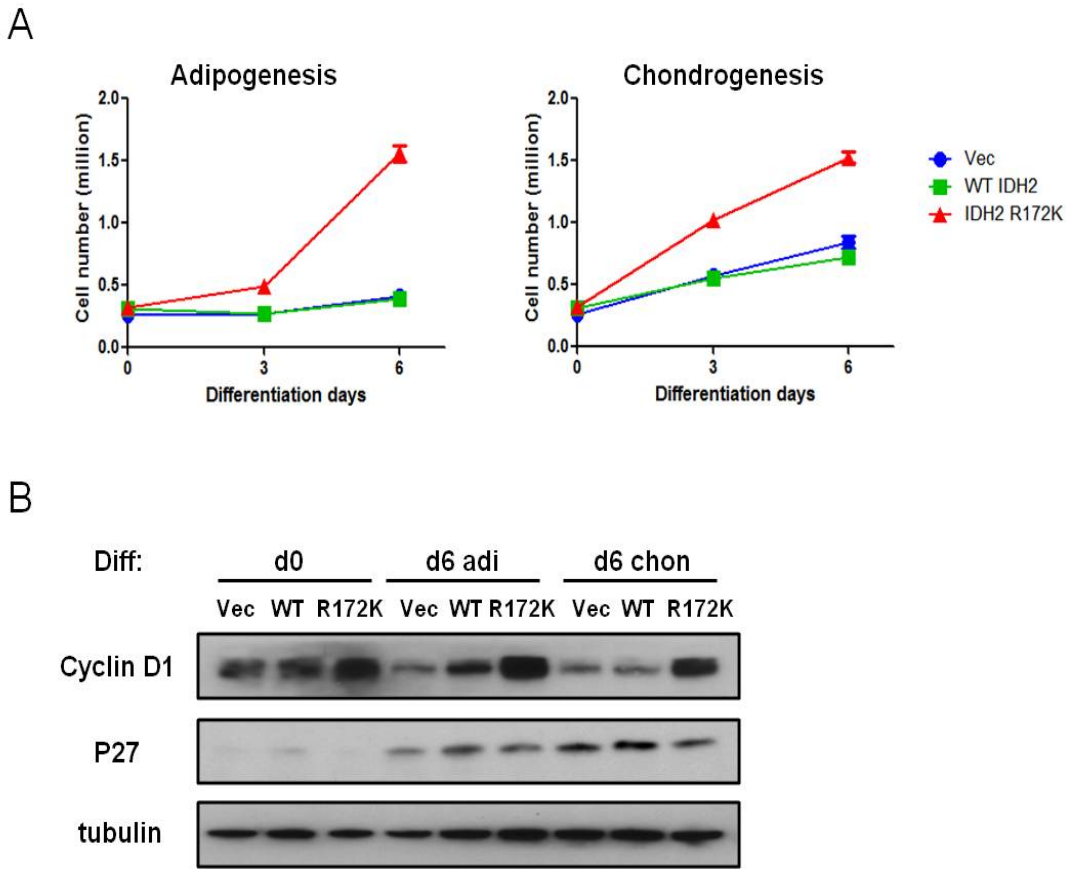

Figure 4.2: Differentiation blockade led to sustained proliferation of IDH mutant cells.

(A) 10T vector, WT or mutant IDH2 cells were treated with adipogenesis or chondrogenesis cocktail. Cell numbers were counted at day 0, 3, 6 after differentiation induction. (B) 10T vector, WT or mutant IDH2 cells were treated with adipogenesis or chondrogenesis cocktail. Six days after differentiation, cells were lysed and protein levels of cyclin D1 and p27 were measured by Western blot.

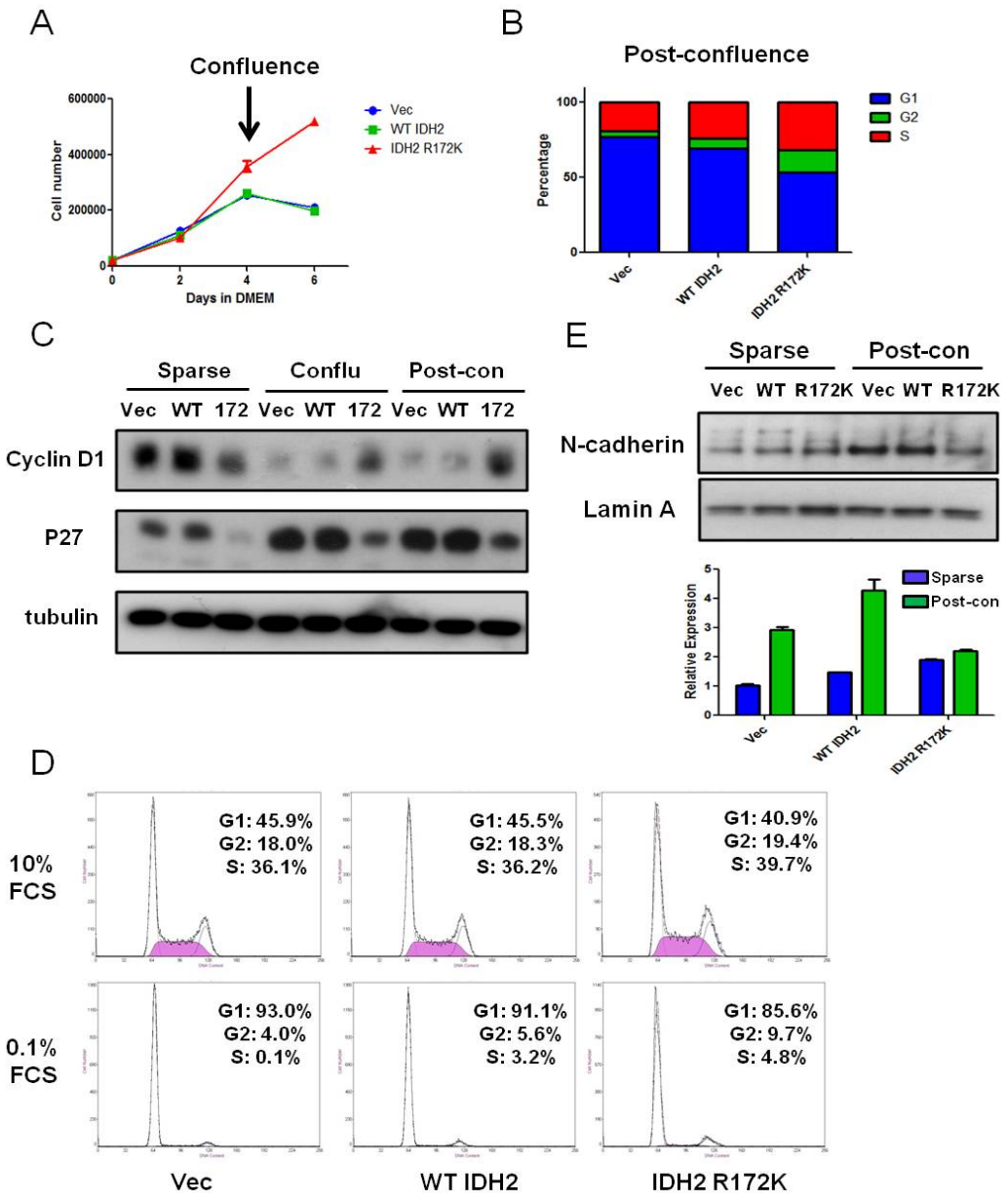

Figure 4.3: IDH mutant cells escape contact inhibition.

(A) 10T vector, WT or mutant IDH2 cells were cultured in normal growth medium and cell numbers were counted at day 0, 2, 4 and 6. Cells reached confluence at day 4. (B) FACS cell cycle analysis of vector, WT or mutant IDH2 cells at post-confluence day 2. (C) Vector, WT or mutant IDH2 cells were lysed at sparse, at confluence or 2 days post-confluence. Protein levels of cyclin D1 and p27 were measured by Western blot. (D) FACS cell cycle analysis of vector, WT or mutant IDH2 cells at sparse in growth medium with 10% or 0.1% fetal calf serum. (E) Vector, WT or mutant IDH2 cells were lysed at sparse or 2 days post-confluence. Levels of N-cadherin protein expression were measured by Western blot and mRNA expression was measured by Q-RTPCR.

(Gumbiner, 2005). We found that unlike vector and WT IDH2 cells, IDH2 mutant cells failed to upregulate N-cadherin protein and mRNA expression after contact inhibition (Figures 4.3E), suggesting that the post-confluence growth of these cells might be the result of inability to sense cell-cell contact at surface membrane.

Since loss of contact inhibition is a classical feature of tumor cells and often indicates transformation, we next tested whether 10T cells with IDH mutation generate tumors *in vivo*. IDH2 mutant cells formed palpable tumors after 20 days of subcutaneous injection and continued to grow up to 1000 m^3, while vector and WT IDH2 cells showed no tumorigenecity over the course of study (Figure 4.4A). Immunohistochemistry staining revealed that IDH2 mutant tumors were highly mitotic with high Ki67 index (Figure 4.4B). Consistent with cell culture study, these tumors also had high levels of cyclin D1 and low p27 expression.

IDH mutation induces DNA hypermethylation

We next sought to determine the mechanism of tumorigenesis by IDH mutation. Previous reports implicate a role of 2HG in inhibiting αKG-dependent chromatin modifying enzymes including TET2 and jumonji-C histone demethylases. These enzymes belong to the superfamily of αKG-dependent dioxgenases, which consist of ~100 members covering diverse biological functions. Among them, 2HG has been proposed to affect activities of prolyl hydroxylases 2 (PHD2) which hydroxylases HIF1α for degradation (Koivunen et al., 2012; Zhao et al., 2009). Moreover, in a knock-in IDH1 mutant mouse model, 2HG was shown to disrupt collagen processing and cause endoplasmic reticulum (ER) stress response by inhibiting collagen prolyl-hydroxylation (Sasaki et al., 2012a).

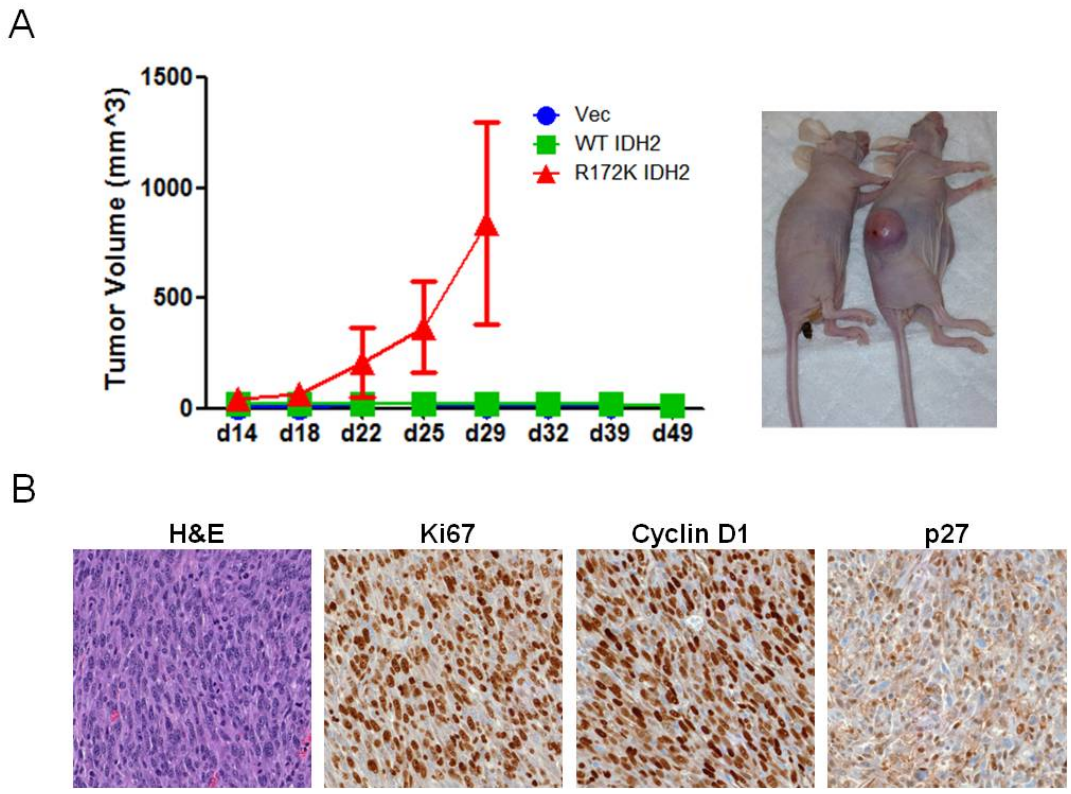

Figure 4.4: IDH mutant cells generate tumors *in vivo*.

(A) 10 millions of 10T vector, WT or mutant IDH2 cells at passage 20 were subcutaneously injected into nude mice. Tumor implantation and growth were monitored and measured. Images are shown for mice injected with WT cells (left) or mutant cells (right). (B) IHC analysis was performed on mutant IDH2 tumors and representative images are shown for H&E, Ki67, cyclin D1 and p27.

We found that soluble fraction of collagen IV seemed to increase in IDH2 mutant cells with a faster migration pattern on SDS gel, suggesting a possible reduced hydroxylation and delayed processing of collagen IV (Figure 4.5A). In addition, we observed a decreased expression of collagen I. However, coating cell culture plates with collagen did not blunt the post-confluence proliferation of mutant IDH2 cells (Figure 4.5B). There was no difference in the levels of ER stress response between IDH2 mutant and WT cells either (Figure 4.5C), suggesting that the mild defect in collagen secretion is unlikely to account for the tumorigenecity of IDH2 mutant cells. Finally, the HIF1α accumulation under hypoxia seemed to be unaffected by IDH2 mutation (Figure 4.5D).

When we extracted DNAs from cells cultured at sparse and subjected them to extended reduced representation bisulfite sequencing (ERRBS) to obtain base-resolution DNA methylation profiles (Akalin et al., 2012), IDH2 mutant cells showed a genome-wide distribution of differentially methylated CpG sites with a profound hypermethylation across all chromosomes (Figure 4.6A). Among the 2,400 genes with differentially methylated cytosines at the promoters, we observed a predominance in hypermethylation which was highly statistical significant (78.1 % being hypermethylated, p-value < 0.0001 by Chi-square test). In contrast, significantly less differentially methylated cytosines were observed between WT IDH2 and vector cells with even distribution of hypermethylated and hypomethylated sites (Figure 4.6B). Pathway enrichment analysis of the hypermethylated sites between IDH2 mutant and WT cells revealed genes involved in cell adhesion and WNT signaling pathways which are implicated in the response to cell-cell contact (Figure 4.6C). Finally, we also found increased methylation at several histone marks such as H3K9me3, H3K9me2 and H3K4me3 in IDH2 mutant cells, which could

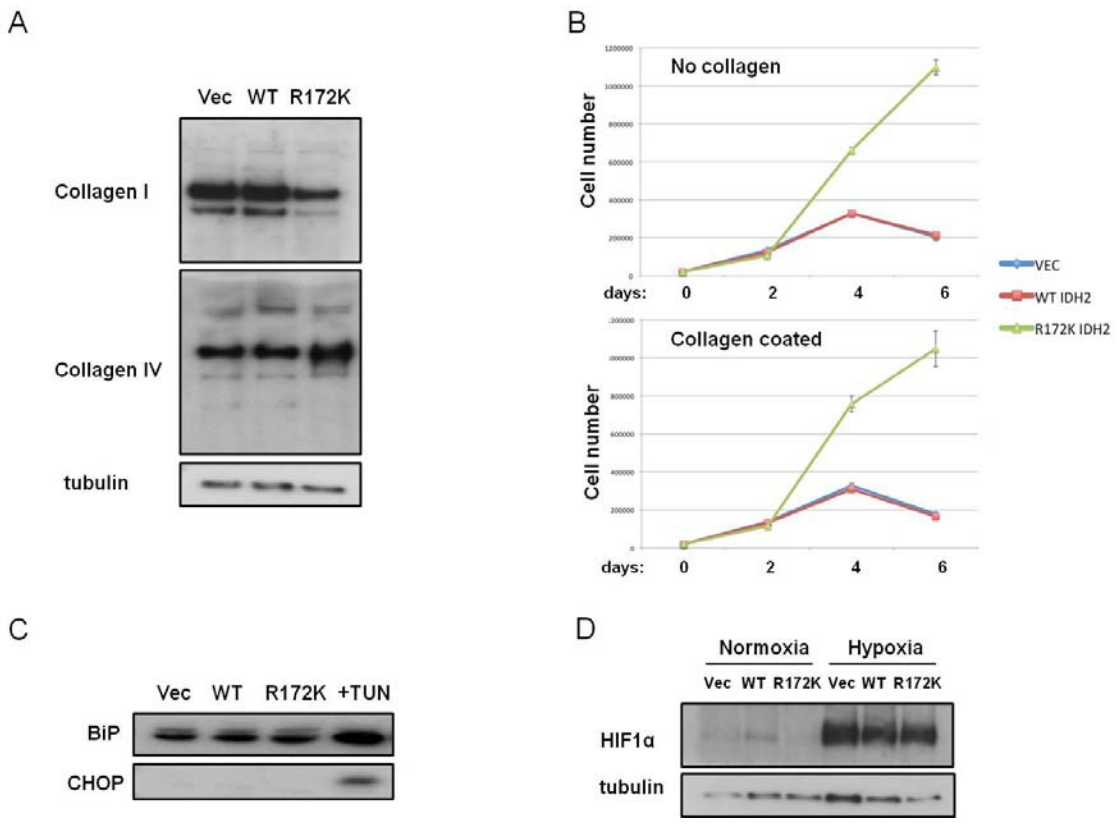

Figure 4.5: Collagen processing and HIF signaling in IDH mutant cells.

(A) 10T vector, WT or mutant IDH2 cells were lysed and protein levels of collagen I and collagen IV in the solution fraction were measured by Western blot. (B) 10T vector, WT or mutant IDH2 cells were seeded on normal cell culture plates or plates coated with collagen and cell numbers were counted at day 0, 2, 4 and 6. Cells reached confluence at day 4. (C) Vector, WT or mutant IDH2 cells and 10T parental cells treated with ER stress inducer tunicamycin were lysed and protein levels of Bip and CHOP were measured by Western blot. (D) Vector, WT or mutant IDH2 cells were lysed under normoxia or after 6 hour under 0.5% hypoxia. Protein levels of HIF1α were measured by Western blot.

reinforce with DNA methylation to modulate gene expression and facilitate the transformation by mutant IDH (Figure 4.6D).

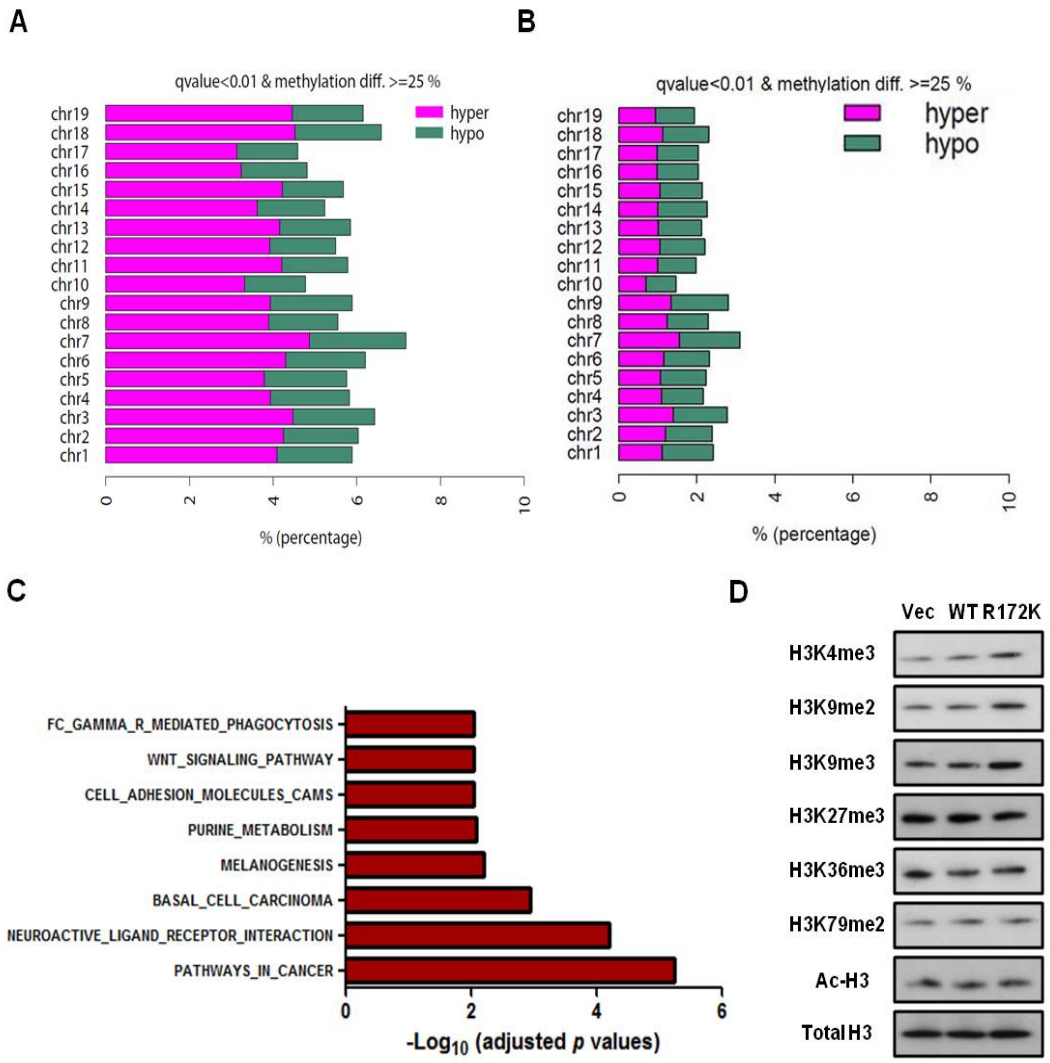

Figure 4.6: IDH mutation induces DNA hypermethylation.

(A) and (B) Stacking barplots showing percentage of hyper and hypomethylated differentially methylated cytosines out of all covered CpGs for each chromosome comparing IDH mutant vs. WT and IDH WT vs. vector. Green represents proportion of hypomethylated cytosines and magenta represents hypermethylated ones. Only CpGs with q-value<0.01 and methylation difference of at least 25% are shown. (C) Pathway enrichment analysis of hypermethylated genes in mutant IDH2 cells. (D) Histones were acid-extracted from vector, WT or mutant IDH2 cells at sparse. Levels of histone methylation were measured by Western blot.

Discussion

The research on IDH mutations has been hampered by a lack of robust model system. We previously found that IDH mutation blocked adipocyte differentiation from mouse fibroblasts (Lu et al., 2012). This finding has been extended to the hematopoietic system with the observations that mutant IDH and 2HG could impair EPO-induced erythrocyte differentiation in an erythroleukemic cell line (Losman et al., 2013) and that hematopoietic-specific conditional knock-in IDH1 R132H mutant mice had an expansion in early haematopoietic progenitor/stem cell population (Sasaki et al., 2012b). Nevertheless, none of the previous studies reported *in vivo* tumorigenecity of mutant IDH, which led to the hypothesis that IDH mutation is insufficient for tumorigenesis. We report here that using a non-transformed murine mesenchymal multipotent cell line, expression of an IDH mutant not only arrested cells from differentiating into adipocytic and chondrocytic lineages, but also resulted in loss of contact inhibition and tumor formation *in vivo*. It should be noted that while differentiation impairment was observed shortly after IDH2 mutant expression, contact inhibition required >15 passages of cells in culture, suggesting that the later phenotype may be the result of gradual epigenetic silencing of key genes involved in cell-cell contact.

The common feature shared by all IDH mutations is the production of 2HG. Although the truncated reverse reaction by mutant IDH also consumes NADPH, its impact on total cellular NADPH pool is likely minimal due to a much slower rate compared to the forward reaction by WT IDH(Dang et al., 2009). Importantly, exogenous 2HG could recapitulate mutant IDH's effect on blocking cell differentiation (Losman et al., 2013; Lu et al., 2012). These data have led to the belief that 2HG is the major mediator of mutant

IDH's oncogenic potential. Despite a strong link between 2HG and αKG-dependent chromatin modifying enzymes, 2HG is a competitive inhibitor for several additional αKG-dependent enzymes *in vitro* (Xu et al., 2011) and in certain context, its impact on enzymes such as prolyl hydroxylases could lead to important biological consequences (Koivunen et al., 2012; Sasaki et al., 2012a). We therefore tested mutant IDH's effect on collagen processing and HIF signaling in our system. The data suggest that HIF signaling was unaffected. Although a mild defect in collagen processing was observed, it did not significantly contribute to the loss of contact inhibition by mutant IDH2. In contrast, DNA methylation profiling at base resolution identified a profound chromosome-wide increase in hypermethylated cytosines in IDH2 mutant cells, presumably due to the inhibition of TET family enzymes. There was also global elevation in histone methylation most likely resulting from 2HG's inhibition of Jumonji-C histone demethylases. Importantly, gene enrichment analysis identified groups of genes involved in contact inhibition that were over-represented in hypermethylated loci. Collectively our findings suggest that chronic inhibition of TET and Jumonji-C histone demethylase may lead to DNA hypermethylation and permanent silencing of genes that are required for proper response to contact inhibition.

There is a strong interest in developing inhibitors that specifically abrogate mutant IDH's ability to produce 2HG. It was shown that 2HG's effect on differentiation arrest could be reversed with delayed kinetics (Losman et al., 2013), suggesting that the epigenetic abnormality is potentially correctable. It remains to be tested, using our model system, whether 2HG is required for tumor initiation and/or maintenance *in vivo*. Given 2HG's

remarkable impact on epigenome, it would also be interesting to test whether compounds targeting chromatin modifiers are selectively toxic to tumors with IDH mutation.

Chapter 5

Discussion and Conclusion

Parts of this chapter have previously been published in: Lu C, Thompson CB. Metabolic regulation of epigenetics. *Cell Metab* 2012 16:9-17.

The epigenetic basis for the oncogenic potential of 2HG-producing IDH mutation

The work presented in this thesis is based on the initial hypothesis that perturbation of an important metabolite αKG's homeostasis can be sensed and responded by cells at the chromatin level. I sought to address the hypothesis by studying the consequence of accumulated 2HG, an αKG structural analogue produced by cancer-associated IDH mutations, on the cellular epigenome. Since IDH mutations are highly prevalent in multiple types of malignancies and are likely to be driver mutations, the model could also help understand how the putative "oncometabolite" 2HG initiates and/or promotes tumorigenesis. I provided several lines of evidence in this thesis supporting the conclusion that not only could 2HG lead to misregulated chromatin modification and remodeling, the resultant epigenetic abnormality also forms the basis for altered cell behavior that are important for tumorigenecity by IDH mutation.

Structural analysis of Jumonji-C histone demethylases reveals that the demethylation reaction requires the coordination of Fe (II) by oxygen atoms in the keto carboxyl end of αKG (Ng et al., 2007). Therefore it is plausible that substitution of one oxygen atom with a hydroxyl group on 2HG may interfere with the reaction efficiency. We and others showed that *in vitro* 2HG is a competitive inhibitor of histone demethylases and TET family 5-methylcytosine hydroxylases (Chowdhury et al., 2011; Lu et al., 2012; Xu et al., 2011). The effective inhibition requires a 2HG:αKG ratio of at least 5:1, suggesting that 2HG is a weak antagonist of these enzymes. However in tumors with IDH mutations, 2HG can accumulate up to 10-50 mM (Dang et al., 2009). Since intracellular concentration of αKG is estimated to be ~1 mM, the amount of 2HG present is sufficient to impair the activity of αKG-dependent chromatin modifying enzymes. In agreement, we

found that ectopic expression of mutant IDH led to remarkable increases in histone and DNA methylation (Figueroa et al., 2010a; Lu et al., 2012). Of note, while transient transfection of mutant IDH in 293T cells enhanced methylation of all histone marks examined, stable expression of mutant IDH over time only resulted in accumulation of specific repressive histone methylation marks such as H3K9me3 and H3K27me3. This could be due to the amount of 2HG produced by different transfection methods and the sensitivity of different Jumonji-C histone demethylases to 2HG inhibition. It could also be explained by the reinforcement between DNA methylation and repressive histone methylation marks. Furthermore, in most cell types tested, the increase in DNA and histone methylation occurred in a passage-dependent manner and could take as long as 10-20 passages. This correlated with the passage-dependent phenotypes induced by mutant IDH reported by us and others (Koivunen et al., 2012; Lu et al., 2012); and as discussed in the following it may provide important insights into the mechanism of hypermethylation establishment.

Multiple independent studies have now demonstrated that differentiation blockade is a hallmark of cells with IDH mutation (Figueroa et al., 2010a; Losman et al., 2013; Lu et al., 2012). This is in agreement with the critical role of epigenetic remodeling in cell lineage specification, as well as the fact that most malignancies involving IDH mutations are characterized by the accumulation of immature cells. Importantly, the differentiation blockade could be phenocopied by exogenous 2HG and depletion of 2HG-inhibitable chromatin modifiers such as TET2 and KDM4C, strongly suggesting that defective chromatin demethylation underlies the inability to execute differentiation. This is further

supported by the findings that key genes required for differentiation but not expressed in IDH mutant cells showed increased levels of repressive H3K9me3 and H3K27me3.

In addition, for the first time we showed that in C3H10T1/2 cells expression of an IDH mutant could lead to tumor formation *in vivo*. Base-resolution DNA methylation profiling revealed a genome-wide CpG hypermethylation which was enriched for genes involved in response to cell-cell contact. Collectively the data presented in this thesis implicate that inhibition of histone and DNA demethylation by 2HG and the resultant changes in gene expression are crucial contributors to the malignant phenotypes induced by mutant IDH. Since chromatin modifications are potentially reversible, it remains to be explored whether modulating chromatin modifying enzymes such as DNA and histone methyltransferases could rescue the phenotypic consequences of IDH mutation.

The present data are supported by findings from patient sample studies. In most cancers involving IDH mutations, the mutations are tightly associated with a CpG island methylator phenotype (CIMP) in patient samples (Figueroa et al., 2010a; Noushmehr et al., 2010; Pansuriya et al., 2011; Wang et al., 2012). Moreover, genetic profiling of AML samples revealed that loss of function mutations of TET2 were mutually exclusive with IDH mutations (Figueroa et al., 2010a). In pediatric and young adult gliomas, genes encoding histone variants H3.3 (*H3F3A*) and H3.1 (*HIST1H3B)* were found to be somatically mutated at specific residues including K27 which appeared to be mutually exclusive with IDH mutations (Schwartzentruber et al., 2012; Wu et al., 2012). These genetic and epigenetic evidence strongly argue that IDH mutations can be grouped with other chromatin mutations and together they constitute disease subgroups characterized

by epigenetic abnormality. Further sequencing efforts in other types of cancer involving IDH mutation are required to generalize these findings.

Mechanisms for establishment of hypermethylation

Recently the genome-wide occupancy of Tet1 was mapped by several groups (Wu and Zhang, 2011). Results showed that Tet1 binds with a high preference for transcription start sites. Moreover, it was found that Tet1 mainly associates with promoters of high CpG content. In progenitor cells, promoters with high CpG content are largely DNA hypomethylated and a significant portion of these promoters are marked by H3K4me3 and H3K27me3. They are enriched for genes involved in regulating differentiation and development. These findings suggest that an important function of Tet1 is to maintain these CpG islands free of methylation by hydroxylating and removing accidental methylation by DNMTs. Since genes showing DNA hypermethylation in cancer tend to be differentiation-related and are marked by H3K4me3 and H3K27me3 in stem cells (Ohm et al., 2007; Widschwendter et al., 2007), poisoning TET's function as a guardian of DNA methylation fidelity may be a potential mechanism to establish DNA hypermethylation in cancer (Williams et al., 2012).

These observations are consistent with the present data and I propose that during differentiation of progenitor cells, Jumonji-C histone demethylase inhibition by the oncometabolite 2HG causes defective histone demethylation and blocks the accessibility of differentiation-related genes. In addition, the inhibition of TET and possibly histone demethylases by 2HG in the long term leads to progressive DNA hypermethylation and permanently "locks" these genes in a silent state. The resulting differentiation arrest may facilitate cancer development through accumulation of undifferentiated cells capable of

self-renewal (Figure 5.1). Future analysis of DNA and histone methylation as well as the genome-wide distribution of jumonji-C histone demethylase /TET bindings will be required to test this hypothesis.

Beyond IDH mutation: crosstalk between metabolism and epigenetics in cancer

The analyses of cancer-associated IDH mutations highlight the dynamics and importance of the interaction between metabolism and epigenetics. As metabolic abnormalities in cancer continue to be uncovered, studies by others have demonstrated additional metabolic perturbations that affect chromatin structure.

Germline mutations in FH and SDH and demethylation of histones and DNA

Germline mutations in the SDHD gene were initially discovered in hereditary paraganglioma through linkage-analysis (Baysal et al., 2000). SDHD gene encodes for a protein that is a part of the mitochondrial succinate dehydrogenase complex (SDH, as known as complex II of the mitochondrial respiratory chain) that generates fumarate from succinate. The mutations were predicted to be loss-of-function. Subsequent sequencing efforts revealed germline mutations of other subunits of the complex II such as succinate dehydrogenase subunit B (SDHB), C (SDHC) and SDH5 in the hereditary paraganglioma and the closely associated phaeochromocytomas (Astuti et al., 2001; Hao et al., 2009; Niemann and Muller, 2000). Mutations in fumarate hydratase (FH, also known as fumarase) were identified as the gene causing hereditary leiomyomatosis and renal-cell cancer syndrome (HLRCC) (Tomlinson et al., 2002). Similar to SDH mutations, mutations in FH are predicted to be loss-of-function. Biochemically, FH catalyzes the enzymatic reaction following SDH, converting fumarate to malate.

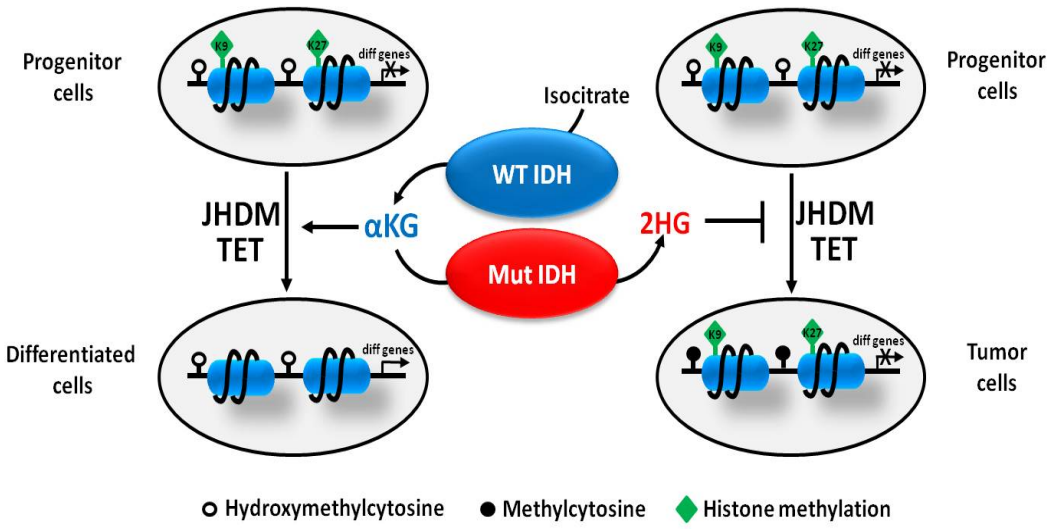

Figure 5.1: Model for 2HG's involvement in epigenetic regulation and cell differentiation.

When progenitor cells differentiate, JHDM removes repressive histone methylation marks (H3K9me3 and H3K27me3) and activates the expression of differentiation-related genes. In addition, TET acts as a failsafe mechanism to protect promoters from aberrant DNA methylation. 2HG produced by mutant IDH inhibits JHDM and TET, which leads to histone and DNA hypermethylation and permanently "locks" differentiation-related genes in a silent state. This results in a differentiation arrest and expansion of progenitor cells, thus facilitating tumor development.

Accumulation of fumarate and succinate as the result of SDH and FH mutations has been proposed to affect HIF signaling as well as the succination of proteins involved in antioxidant response (Adam et al., 2011; Isaacs et al., 2005; Selak et al., 2005). Given that structurally both fumarate and succinate are similar to αKG and 2HG, one would expect that SDH and FH mutations may also affect αKG-dependent chromatin modifying enzymes. Indeed, it was shown that *in vitro* and in cells fumarate and succinate can broadly inhibit αKG-dependent Jumonji-C histone demethylases and TET family enzymes (Xiao et al., 2012). The functional consequences of these inhibitions remain unexplored especially in relation to HIF signaling, since unlike cancers with IDH mutations, paraganglioma, phaeochromocytomas and renal-cell cancers typically exhibit extensive angiogenesis and vascularization, suggesting the activation of the HIF pathway.

Methionine metabolism and methylation

DNA methyltransferase (DNMTs) and histone methyltransfersase (HMTs) add methyl groups to DNA or lysine/arginine residues of histones, respectively. Although structurally diverse and possessing high substrate specificities, DNMTs and HMTs share a similar reaction mechanism: transferring a methyl group from S-adenosyl methionine (SAM) to the substrate with the formation of the by-product S-adenosyl homocysteine (SAH). Since SAH is a very potent inhibitor of DNMTs and HMTs, the key metabolic determinant of methyltransferase reactions is the ratio between SAM and SAH and rate of SAH clearance which both depend on the supply of methyl group by various donors.

A recent report identified overexpression of nicotinamide N-methyltransferase (NNMT) in a variety of human cancers (Ulanovskaya et al., 2013). NNMT also converts SAM to

SAH, but transfer the methyl group to 1-methylnicotinamide instead of protein or DNA. It was shown that overexpression of NNMT consumes the methyl unit pool in cells and as a result decreases the reaction efficiency of HMT and leads to histone hypomethylation.

Interestingly, mouse embryonic stem cells are highly dependent on extracellular levels of threonine (Wang et al., 2009). It was recently shown that threonine's importance was due to the supply of most methyl units used for histone methylation by its catabolism (Shyh-Chang et al., 2013). Cells deprived of theronine showed dramatic decrease in H3K4me3. The catabolic pathway for threonine is absent in human. For proliferating cells in human the most likely source of methyl units comes from serine/glycine catabolism. Intriguingly, the key enzyme in serine metabolism pathway, phosphoglycerate dehydrogenase (PHGDH), was found to be amplified in melanoma and breast cancer (Locasale et al., 2011; Possemato et al., 2011). It is yet to be shown whether PHGDH amplification could potentially modulate the cellular methylome and the epigenetic state.

Concluding remarks

The present data demonstrate that the disturbance of αKG homeostasis through IDH mutation led to altered cellular response to environment trigger, implying that proper balance of intracellular metabolite levels is a prerequisite for the precise execution of cell fate specification. Therefore it appears that a "metabolic checkpoint" exists for cells to determine the nutrient availability in the microenvironment before engaging in fate decision process. Furthermore, covalent modifications of histone tails and DNA such as methylation are likely mechanisms to sense and memorize the metabolic state of the cell.

As many complex diseases such as cancer and type II diabetes display abnormalities of cellular metabolism and epigenome, it will be critical to understand how cells coordinate signal transduction and metabolic flux to control chromatin remodeling and gene expression.

Research on metabolism and epigenetics are progressing at an unprecedented pace and more exciting discoveries are anticipated to arrive over the near future. Yet technological challenges are present that must be overcome to unravel the mystery at the next level. As most metabolites are not diffusible between mitochondria and cytosol/nucleus, accurate determination of the cytoplasmic pool size is critical to understand their effects on epigenetic signaling. Although attempts have been made, so far the technology to reliably measure metabolite concentrations in different cellular compartments is lacking. Even within the same compartment, local concentration of the metabolite may vary, as substrate channeling is a common event in cellular metabolism (Huang et al., 2001). This is relevant, as metabolic enzymes are often present in transcriptional complexes, and thus could provide a local supply of substrates/co-factors to the complexes in which they localize. For example, methionine adenosyltransferase IIα (MATIIα), which generates SAM, was present in chromatin-associated complexes and thought to provide local substrate for methyltransferases reactions (Katoh et al., 2011). Alternatively metabolic enzymes may function in these complexes independently of their metabolic activity (Tristan et al., 2011; Yang et al., 2011). Finally, system biology approaches will become increasingly important to fully grasp the complexity of the connections between metabolism and chromatin dynamics. A deeper understanding of these connections may

help shed light on our understanding of the etiology of a variety of complex diseases (Katada et al., 2012; Sahar and Sassone-Corsi, 2012).

Appendix
Materials and Methods

Statistical Analysis: Statistical analysis of demographic factors, disease characteristics, and mutational frequencies was performed using Fisher's exact test and Chi-square tests for categorical variables and t-tests and Mann-Whitney U test for continuous variables. Statistical analysis for other experiments was performed using Student's t-test (two sample equal variance; two-tailed distribution).

Plasmid construction: The cDNA clone of human IDH1 (BC012846.1) was purchased from ATCC in pCMV-Sport6, and human IDH2 (BC009244) was purchased from Invitrogen in pOTB7. Standard site-directed mutagenesis techniques were used to generate IDH1 R132H by introducing a g395a base pair change in the IDH1 open reading frame (ORF). IDH2 R172K was made by introducing a g515a change in the IDH2 ORF, while IDH2 R140Q was made with a g419a alteration. Wild-type and mutant sequences were then subcloned into LPC vector or MIGR1 vector. TET2 cDNA was synthesized and subcloned into pCMV6-ENTRY (Origene) with a C-terminal FLAG tag and myc tag. All sequences were confirmed by direct sequencing before expression in 293T cells and retrovirus generation.

Cell culture, transfection/transduction, and generation of stable cell lines: 293T, NHA cells immortalized by E6/E7/hTERT (kindly provided by Russ Pieper/UCSF), C3H10T1/2 and 3T3-L1 cells were cultured in Dulbecco's modified Eagle's medium (DMEM, Invitrogen) with 10% fetal bovine serum (FBS, CellGro). 32D cells were cultured in RPMI-1640 medium (Invitrogen) supplemented with 10% fetal bovine serum

and 3 ng/ml recombinant IL-3 (BD Biosciences, 554579). For expression of TET2 cDNA, TET2 shRNAs, and wild-type and mutant IDH1/2 in 293T cells, transfection was performed with Lipofectamine 2000 (Invitrogen) according to the manufacturer's instructions. For generation of IDH2 retrovirus, TET2 shRNA retrovirus and transduction of 32D and mouse primary bone marrow cells, supernatant from 293T cells transfected with pCL-Eco helper virus and plasmids was collected after 72 h, filtered and applied to cells overnight. For generating 32D cell lines with stable expression of wild-type or mutant IDH2, cells were grown in 2.5 μg/ml puromycin for 7 days following LPC retroviral transduction. Pooled populations of puromycin-resistant cells were obtained, and then continuously cultured in puromycin.

For generation of IDH2 retrovirus and transduction of 3T3-L1 and 10T1/2 cells, supernatant from 293T cells transfected with pCL-Eco helper virus and plasmids was collected after 72 h, filtered and applied to cells overnight. For generating 3T3-L1 and 10T1/2 cell lines with stable expression of wild-type or mutant IDH2, cells were grown in 2.5 μg/ml puromycin for 7 days following retroviral transduction. Pooled populations of puromycin-resistant cells were obtained, and then continuously cultured in puromycin.
For generation of IDH1 retrovirus and transduction of NHA cells, GP2-293 cells (Clontech, 631458) were calcium phosphate transfected with equal amounts of pVSV-G (Clontech, 631512) and plasmids. Virus was harvested at day 2 and day 3 after transfection and placed on logarithmically growing cells. After infection, cells were placed in 800 μg/mL G418 (Invitrogen) to generate stable cell lines.
For siRNA knockdown of KDM4C, transfections were performed with Lipofectamine RNAiMAX (Invitrogen), using siRNAs targeting KDM4C (#1: sense 5'-

GCUUGAAUCUCCCAAGAUAtt-3' antisense 5'-UAUCUUGGGAGAUUCAAGCtt-3'; #2: sense 5'-CAAAGUAUCUUGGAUCAAAtt-3' antisense 5'-UUUGAUCCAAGAUACUUUGcc-3'; #3: sense 5'-GAGGAGUUUCGGGAGUUCAACAAAU-3' antisense 5'-AUUUGUUGAACUCCCGAAACUCCUC-3') or a non-targeting control (Dharmacon, #D-001810-01-20) at a concentration of 40 nM.

Tet2 shRNA experiments: Oligonucleotide sequences targeting murine Tet2 (NM_001040400) were selected on the basis of BIOPREDsi algorithms and are available upon request. Individual shRNAs for validation were synthesized as 97 bp oligos (Sigma Genosys), PCR-amplified, cloned into LMS (MSCV-based vectors encoding GFP), and verified by sequencing. Tet2 KD was verified by qRT-PCR using SYBR green quantification in an ABI 7500 sequence detection system. The following primers for Tet2 were used to verify KD: Forward 5'-CAAAGATGAAGCTCCTTATTATACC-3'; Reverse 5'-ACATCCCTGAGAGCTCTTGC-3'.

Immunofluorescence staining and quantification: Cells were seeded in Lab-tech II 4-wells chamberslides (Electron Microscopy Sciences) after transfection. After wash with PBS, cells were fixed with paraformaldehyde (3%) for 10 min at room temperature and permeabilized with 0.2% Triton X-100 for 20 min. Cells were then treated with 2N HCL for 30 min at room temperature and subsequently neutralized with 100 mM Tris-HCL, pH 8.0. After wash with PBS, blocking solution (1% BSA in PBS) was added for 30 min at room temperature followed by incubation with anti-FLAG antibody (1:1000, Sigma, F1840) or anti-5-OH-methylcytosine antibody (1:2000, Active Motif, 39770) overnight at 4°C. Secondary antibodies coupled with ALEXA FLUOR® 488 or Cy3 (Invitrogen)

were used to detect fluorescence signal. After wash with PBS, samples were stained in DAPI for 30 s and mounted in Prolong Gold antifade reagent (Invitrogen, P36934).

Cytosine modification measurement by LC-ESI-MS/MS system: DNA hydrolysis was performed as previously described (Song et al., 2005). Briefly, one microgram of genomic DNA was first denatured by heating at 100 ^{o}C. Five units of Nuclease P1 (Sigma, Cat # N8630), was added and the mixture incubated at 37 ^{o}C for 2 hours. A 1/10 volume of 1 M Ammonium bicarbonate and 0.002 units of venom phosphodiesterase 1 (SIGMA, Cat # P3243) were added to the mixture and the incubation continued for 2 hours at 37 ^{o}C. Next, 0.5 units of Alkaline phosphatase (Roche, Cat # 108138) was added and the mixture incubated for 1 hour at 37 ^{o}C. Before injection into an Agilent zorbax 4.6mmx50mm, 3.5um particle size -c18 column, the reactions were diluted with water to dilute out the salts and the enzymes. LC separation was performed at a flow rate of 220 L/min. Quantification was done using a LC-ESI-MS/MS system in the multiple reaction monitoring (MRM) mode as described (Song et al., 2005).

AML patient samples and sequence analysis: AML blasts, which had been enriched from either peripheral blood or bone marrow samples by Ficoll centrifugation and frozen viable, were obtained from the ECOG sample bank. Samples were analyzed under light microscopy and found to be >90% blasts after thawing. The ECOG's Cytogenetic Subcommittee reviewed conventional chromosome studies that were obtained by individual institutions and categorized patients as having a risk profile that was favorable, unfavorable, intermediate, or indeterminate on the basis of a published classification system. All patients were tested centrally for the most common AML molecular aberrations, including the mixed-lineage leukemia gene (MLL), partial tandem

duplication (PTD), and FMS-like tyrosine kinase 3 (FLT3)–internal tandem duplication (ITD), with the use of a semiquantitative polymerase-chain-reaction (PCR) assay.

Genomic DNA was extracted from bone marrow and/or peripheral blood mononuclear cells from AML patients in the ECOG 1900 cohort at diagnosis. High-throughput DNA sequence analysis was used to screen for FLT3, NPM1, CEBPA, H/K/NRAS, KIT, WT1, TET2, ASXL1, IDH1/2, TP53, RUNX1, PTEN, and PHF6 in pre-treatment genomic DNA. All DNA samples were whole genome amplified using Ø29 polymerase and mutations were validated on unamplified DNA to ensure all mutations were present in the diagnostic sample. We performed high throughput PCR amplification followed by DNA sequence analysis using an ABI 3730 capillary sequencer (Agencourt Bioscience, Beverly, MA). Bidirectional sequence traces were analyzed for mutations using Mutation Surveyor (Softgenetics, Inc., State College, PA), and all traces with putative mutations were reviewed manually. Samples with missense alleles reported as germline alleles in dbSNP (dbSNP, http://www.ncbi.nlm.nih.gov/projects/SNP) were censored from analysis. Mutations were scored as somatic based on sequence analysis of matched remission DNA or based on prior paired sample sequencing demonstrating specific alleles are somatic; missense alleles which could not be shown to be somatic were censored from analysis; as with previous studies all frameshift and nonsense alleles were somatic in origin. All somatic mutations were validated by resequencing non-amplified source DNA for the particular amplicon where the mutation was noted. Visual representation of sequencing data for TET2 and IDH1/2 mutations was performed by creating a Circos diagram.

Histone extraction and Western blotting: For histone acid-extraction, cells were lysed in hypotonic lysis buffer (10 mM HEPES, 10 mM KCl, 1.5 mM $MgCl_2$, 0.5 mM DTT, protease inhibitors) for 1 h. H_2SO_4 was added to 0.2 N for overnight at 4^oC with rotation. After spinning down and collecting supernatant, proteins were precipitated in 33% TCA, washed with acetone, and resuspended in deionized water. For whole cell lysate, cells were lysed in standard RIPA cbuffer (1% NaDOC, 0.1% SDS, 1% TritonX-100, 0.01 M Tris pH 8.0, and 0.14 M NaCl), and lysates were then centrifuged at 14,000 g at 4ºC. Supernatants were collected and normalized for total protein concentration, then separated by SDS-PAGE, transferred to nitrocellulose membrane, blocked in 5% non-fat milk in PBS-0.5% Tween-20, and probed with primary antibodies, and detected with horseradish peroxidase-conjugated anti-rabbit or anti-mouse secondary antibodies (GE Healthcare, NA934V and NA931V). Primary antibodies used include: anti-IDH1 (Proteintech, 12332-1-AP), anti-IDH2 (Abcam, ab55271), anti-GST tag (Millipore, 05-311), anti-H3K9me2 (Cell Signaling Tech, 9753), anti-H3K9me3 (Abcam, ab8898), anti-H3K36me3 (Abcam, ab9050), anti-H3K27me3 (Millipore, 17-622), anti-H3K4me3 (Millipore, 17-614), anti-H3K79me2 (Cell Signaling Tech, 9757), anti-KDM4C (Abcam, ab85454), anti-acetyl H3 (Upstate, 06-599), anti-H3 (Cell Signaling Tech, 4499), anti-tubulin (Sigma, T9026), anti-GFAP (Cell Signaling Tech, 3670), anti-β3-tubulin (Cell Signaling Tech, 5666), anti-p85 (Millipore, 06-195), anti-nestin (Millipore, MAB5326), anti-β-actin (Sigma, A5316), anti-cyclin D1 (EMD, CC12), anti-p27 (Santa Cruz Biotechnology, sc-1641), anti-N-cadherin (Cell Signaling Tech, 4061), anti-Collagen I (Abcam, ab21286), anti-Collagen IV (Abcam, ab6586), anti-BiP (Cell Signaling Tech, 3177), anti-CHOP (Cell Signaling Tech, 2895) and anti-HIF1α (Cayman Chemical,

10006421). Anti-IDH1 R132H mutant antibody was a kind gift from Agios Pharmaceuticals. Quantification of Western blot band intensity was performed using Image J software according to manufacturer's instruction.

Metabolite extraction and GC-MS analysis: After gentle removal of culture medium, cells were rapidly quenched with ice cold 80% methanol and incubated at -80ºC for 20 min. Following sonication, extracts were then centrifuged at 14,000 g for 20 min at 4ºC to remove precipitated protein, and the aqueous metabolites in the supernatant layer were dried under nitrogen gas. For GC-MS analysis, dried extracts were redissolved in a 1:1 mixture of acetonitrile and N-methyl-N-*tert*-butyldimethylsilyltrifluoroacetamide (MTBSTFA; Regis) and heated for 75 min at 70ºC to derivatize metabolites. Samples were then injected into an Agilent 7890A GC with an HP-5MS capillary column, connected to an Agilent 5975 C mass selective detector operating in splitless mode using electron impact ionization with ionizing voltage of -70 eV and electron multiplier set to 1060 V. GC temperature was started at 100ºC for 3 min, ramped to 230ºC at 4ºC/min and held for 4 min, then ramped to 300ºC and held for 5 min. Mass range of 50-500 amu was recorded at 2.71 scans/s. Identification of the 2HG metabolite peak was confirmed using standards obtained from Sigma. 2HG and glutamate signal intensities were quantified by integration of peak areas.

Flow cytometry: For cell surface staining of C-Kit, 1 x 10^6 32D cells were used for each condition. After wash with PBS, cells were incubated for 15 min with anti-C-Kit antibody conjugated with APC (1:100, BD Biosciences, 553356). Cells were then washed 3 times in PBS and analyzed by Becton Dickinson Calibur flow cytometer. For intracellular staining of FLAG and 5-OH-methylcytosine, 5 x 10^6 293T cells were used

for each condition. After wash with PBS, cells were fixed with paraformaldehyde (3%) for 10 min at room temperature and permeabilized with 0.5% Triton X-100 for 10 min. Cells were then treated with 2N HCL for 20 min at room temperature and subsequently neutralized with 100 mM Tris-HCl, pH 8.0. After wash with PBS, cells were incubated with anti-FLAG (1:200) and anti-5-OH-methylcytosine (1:400) antibodies for 30 min at room temperature. After wash with PBS, cells were incubated with secondary antibodies coupled with ALEXA FLUOR® 488 or Cy5 (Invitrogen) for 30 min in the dark. Cells were then washed 3 times in PBS and analyzed by Becton Dickinson Calibur flow cytometer. Data analysis was done using CellQuest.

For FACS analysis of cell cycle distribution, adherent cells in a six-well plate were trypsinized and collected in 15-ml centrifuge tubes. The collected cells were fixed by ethanol (final concentration of 70%) overnight at -20 ºC. Cells were then stained with 50 µg/ml propidium iodide (Sigma) with 0.1 mg/ml RNase A for 40 min at 37 ºC. After washing with PBS, the DNA content of the stained cells was then analyzed by Becton Dickinson Calibur flow cytometer.

Glioma patient samples, mutational analysis, microarray and gene ontology functional analysis: Primary oligodendroglioma samples were obtained with approval from the institutional review board at the University of Pennsylvania and were de-identified for the study. For microarray analysis, tumor sample RNA was extracted with Trizol and purified with Qiagen RNeasy, and then assayed on an Affymetrix Human Gene 1.0ST array. "Significance Analysis of Microarrays" (http://www-stat.stanford.edu/~tibs/SAM/sam.pdf) was applied to find differentially expressed genes (q-value < 10% and fold-change >2). Functional analysis of differentially expressed

genes was done using the DAVID tool (http://david.abcc.ncifcrf.gov/home.jsp) using all human genes as a background set.

For IDH mutation analysis, tumor genomic DNA was extracted and the regions surrounding IDH1 codon 132 and IDH2 codons 140 and 172 were amplified by PCR followed by sequencing. IDH1 analysis used forward primer 5'-ACCAAATGGCACCATACGA-3' and reverse primer 5'-TTCATACCTTGCTTAATGGGTGT-3' for amplification, and primer 5'-CGGTCTTCAGAGAAGCCATT-3' for sequencing[1]. IDH2 analysis used forward primer 5'-CAGAGACAAGAGGATGGCTAGG-3' and reverse primer 5'-GTCTGCCTGTGTTGTTGCTTG-3' for amplification, and the same forward primer for sequencing[27]. Out of the 42 tumors analyzed, 41 had sufficient high quality genomic DNA for discerning IDH mutation status. The one sample unable to be classified as either IDH wild-type or mutant was excluded from further analysis.

Cell differentiation and Oil-red O staining: 3T3-L1 cell differentiation and Oil-red O staining were carried out as described previously (Wellen et al., 2009). In brief, confluent 3T3-L1 cells were stimulated with a cocktail containing 0.5 mM isobutylmethylxanthine, 1 μM dexamethasone, 5 μg/ml insulin, and 5 μM troglitazone (all from Sigma) in DMEM with 10% FBS, to induce differentiation. Cells were maintained in DMEM with insulin after two days of differentiation until ready to be harvested. For Oil-red O staining, cells were washed in PBS and then fixed for 20 min at room temperature with 3% paraformaldehyde. Cells were then washed with deionized water and stained with Oil-red O solution. For quantification, O-red O staining was dissolved in isopropanol and absorbance was measured at 500 nm.

Adipocyte differentiation of 10T1/2 cells was done following the same procedure as 3T3-L1 cells. Chondrocyte differentiation of 10T1/2 cells was performed as previously described (Mikami et al., 2011). In brief, confluent 10T1/2 cells were stimulated with a cocktail containing DMEM with 1% FBS, 10 μg/mL human insulin (Sigma), 3×10^{-8} M sodium selenite (Sigma), 10 μg/mL human transferrin (Sigma), 10^{-8} M dexamethasone, and 100 ng/mL rhBMP-2 (R&D system). Medium were replaced with fresh cocktail every 2-3 days until cells were ready to be imaged or harvested.

***In vitro* histone demethylase assay:** The histone demethylase assay was carried out as described previously (Ingvarsdottir et al., 2007). In brief, 4 μg bulk calf thymus histones (Sigma) were incubated with GST-tagged KDM4C (1.42 μg, BPS Bioscience) in a reaction mix containing 50 mM Tris-HCl pH 8.0, protease inhibitors cocktail, 1 mM αKG, 100 μM $FeSO_4$ and 2 mM ascorbic acid at 37 °C for 4 h, in the absence or presence of various concentrations of D-2HG or L-2HG (Sigma). Reaction mixtures were analyzed by Western blotting using specific antibodies.

Quantitative real-time PCR: RNA was isolated using Trizol (Invitrogen). After incubating with DNase, cDNA was synthesized using Superscript II reverse transcriptase (Invitrogen). Quantitative PCR was performed on a 7900HT Sequence Detection System (Applied Biosystems) using Taqman Gene Expression Assays (Applied Biosystems). Gene expression data was normalized to 18S rRNA.

Chromatin immunoprecipitation assay: Chromatin immunoprecipitation assay was performed with Millipore Magna ChIP™ G kit (Millipore, 17-611). In brief, two million cells were cross-linked with 1% formaldehyde for 10 min at room temperature. After

washing with cold PBS, cells were centrifuged and lysed in 500 µl SDS lysis buffer for 10 min on ice. Lysate was then sonicated using Bioruptor® sonicator (Diagenode) to shear DNA to approximately 200-600 bp. Samples were spun down and 50 µl of the supernatant were used for each immunoprecipitation overnight with magnetic beads after 10 x dilution. Primary antibodies (3 µg per ChIP) used were: anti-H3K9me3 (Abcam, ab8898) and anti-H3K27me3 (Millipore, 17-622). Normal rabbit IgG (Millipore, 12-370) was used as control and showed minimal enrichment. The next day, samples were washed in low salt immune complex buffer, high salt immune complex buffer, LiCl immune complex buffer, and TE buffer. Histone complexes were eluted in elution buffer plus proteinase K for 2 h at 65ºC. DNA was recovered using columns. Quantitative PCR was performed on purified DNA samples. Primers used are: *Adipoq* forward: 5'-ATGGCTGAACCACACAGCTTCA-3', reverse: 5'-AGGGGTCAGGAGACCTCCCTTT-3'; *Cebpa* forward: 5'-CTGGAAGTGGGTGACTTAGAGG-3', reverse: 5'-GAGTGGGGAGCATAGTGCTAG-3'. Data points (Ct) are converted to percentage of input.

Quantitative DNA methylation analysis by MassARRAY EpiTyping: Matrix-assisted laser desorption/ionization time-of-flight mass spectrometry using EpiTyper by MassARRAY (Sequenom) was performed on bisulfite-converted DNA extracted from 3T3-L1 cells. MassARRAY primer design was done as previously described (Figueroa et al., 2009).

Immunohistochemistry: The immunohistochemistry detection was performed using Discovery XT processor (Ventana Medical Systems). The tissue sections were blocked

for 30 min in 10% normal goat serum in 0.2% BSA/PBS, followed by incubation for 5 h with 0.1 µg/ml of the rabbit polyclonal anti-H3K9me3 (Abcam, ab8898) or 1 µg/ml rabbit polyclonal anti-H3K27me3 (Millipore, 07-449) antibodies and incubation for 60 min with biotinylated goat anti-rabbit IgG (Vector labs, PK6101) at 1:200 dilution. The detection was performed with DAB-MAP kit (Ventana Medical Systems). The entire slides were scanned by Zeiss Mirax Scan (Carl Zeiss) using 20x/0.8 objective. The scanned image was exported into image analysis software, Metamorph (Molecular Devices). Color threshold for DAB-positive nuclei was determined and set for all images. Areas above threshold for DAB signal and for hematoxylin-counter stained total nuclei were measured in an automated fashion. Ratio between the two parameters were calculated and analyzed for statistical significance.

Synthesis of 1-octyl-D-2-hydroxyglutarate: Commercial *R*(-)-tetrahydro-5-oxofuran-2-carboxylic acid (140 mg, 1.076 mmol) was dissolved in H_2O (1 ml), cooled to 0^oC and treated with 1 N KOH (2.16 ml, 2.15 mmol). The resulting solution was stirred at this temperature for 5 min and at ambient temperature for 2 h. It was then concentrated to dryness under reduced pressure and dried. The residue was dissolved in trifluoroacetic anhydride (8 ml) at 0^oC, stirred for 30 min at 0^oC, 2 h at room temperature, then the volatiles were evaporated under reduced pressure. The residue was dried and dissolved in anhydrous tetrahydrofuran (6 ml). Octanol (0.3 ml, 2.1 eq.) was added to the solution at 0^oC and the mixture was stirred for an overnight period at ambient temperature. Water was added to quench the reaction, and the mixture extracted with EtOAc. The combined extracts were dried over $MgSO_4$, concentrated and purified by Flash chromatography (EtOAc/Hexane 1:3 and 1:1) to give 1-octyl-D-2-hydroxyglutarate (110 mg, 39%).

Neurosphere isolation, culture and differentiation: Six days postpartum Ink4a/Arf null ($p16/p19^{-/-}$) mice were sacrificed with the isolated subventricular zones subjected to chemical (Pronase E, Calbiochem 7433-2) and mechanical dissociation to obtain a single cell suspension in full neurobasal medium (Neurobasal medium, GIBCO 21103; B27 supplement without retinoic acid, GIBCO 12587-010; Glutamax, GIBCO 35050; 20 ng/mL EGF, R&D Systems 236-EG; 20 ng/mL basic FGF, Millipore GF003). On the next day the cells were spun down and re-suspended in fresh medium, and once neurospheres had formed in culture, the spheres were collected and chemically dissociated (Accumax, Innovative Cell Technologies AM105) back into single cells in fresh medium.

One day after final infection, infected neurospheres and a non-infected control were placed in 400 µg/mL Hygromycin B (InvivoGen, ant-hg-1). Once selection was complete, isogenic cell lines maintained in full neurobasal medium were chemically dissociated into single cells and were plated at the same density in full neurobasal medium with increasing concentrations of retinoic acid (Sigma-Aldrich, R2625). 72 h later cells were harvested, and expression of proteins was analyzed by Western blotting.

Measurement of total CpG methylation: DNA methylation was assessed as previously described (Habib et al., 1999). In brief, 1 x 10^6 NHA cells were washed with PBS and fixed with 2% paraformaldehyde for 10 min at room temperature and permeabilized with 0.5% Triton X-100 for 10 min. Cells were then treated with 2 N HCL for 20 min at room temperature and subsequently neutralized with 100 mM Tris-HCl, pH 8.0. Cells were incubated with anti-5-methylcytosine antibody (Calbiochem, NA 81) at 1:100 dilution for 30 min at room temperature. After washing with PBS, cells were incubated with

secondary antibody coupled with ALEXA FLUOR® 488 (Invitrogen) for 30 min in the dark. Flow cytometry was done using Becton Dickinson Calibur flow cytometer and analyzed using FlowJo software.

Tumor xenograft study: 10T1/2 cells were harvested with trypsin and resuspended in PBS. About 10^7 cells were injected s.c. into both flanks of 6-8 weeks old athymic female nude mice (Jackson Lab). Formation of tumors was monitored. After tumors became palpable, tumor volumes were estimated by caliper measurements assuming spherical geometry (volume = $d^3 \times \pi/6$).

Extended reduced representation bisulfite sequencing (ERRBS): Genomic DNA was extracted from 10T1/2 cells with Qiagen Gentra Puregene kit. ERRBS was performed with 25-50ng genomic DNA as described previously (Akalin et al., 2012).

Bibliography

Abdel-Wahab, O., Mullally, A., Hedvat, C., Garcia-Manero, G., Patel, J., Wadleigh, M., Malinge, S., Yao, J., Kilpivaara, O., Bhat, R., *et al.* (2009). Genetic characterization of TET1, TET2, and TET3 alterations in myeloid malignancies. Blood *114*, 144-147.

Adam, J., Hatipoglu, E., O'Flaherty, L., Ternette, N., Sahgal, N., Lockstone, H., Baban, D., Nye, E., Stamp, G.W., Wolhuter, K., *et al.* (2011). Renal cyst formation in Fh1-deficient mice is independent of the Hif/Phd pathway: roles for fumarate in KEAP1 succination and Nrf2 signaling. Cancer Cell *20*, 524-537.

Akalin, A., Garrett-Bakelman, F.E., Kormaksson, M., Busuttil, J., Zhang, L., Khrebtukova, I., Milne, T.A., Huang, Y., Biswas, D., Hess, J.L., *et al.* (2012). Base-pair resolution DNA methylation sequencing reveals profoundly divergent epigenetic landscapes in acute myeloid leukemia. PLoS Genet *8*, e1002781.

Amary, M.F., Bacsi, K., Maggiani, F., Damato, S., Halai, D., Berisha, F., Pollock, R., O'Donnell, P., Grigoriadis, A., Diss, T., *et al.* (2011). IDH1 and IDH2 mutations are frequent events in central chondrosarcoma and central and periosteal chondromas but not in other mesenchymal tumours. J Pathol *224*, 334-343.

Astuti, D., Latif, F., Dallol, A., Dahia, P.L., Douglas, F., George, E., Skoldberg, F., Husebye, E.S., Eng, C., and Maher, E.R. (2001). Gene mutations in the succinate dehydrogenase subunit SDHB cause susceptibility to familial pheochromocytoma and to familial paraganglioma. Am J Hum Genet *69*, 49-54.

Baylin, S.B., and Jones, P.A. (2011). A decade of exploring the cancer epigenome - biological and translational implications. Nat Rev Cancer *11*, 726-734.

Baysal, B.E., Ferrell, R.E., Willett-Brozick, J.E., Lawrence, E.C., Myssiorek, D., Bosch, A., van der Mey, A., Taschner, P.E., Rubinstein, W.S., Myers, E.N., *et al.* (2000).

Mutations in SDHD, a mitochondrial complex II gene, in hereditary paraganglioma. Science *287*, 848-851.

Bilodeau, S., Kagey, M.H., Frampton, G.M., Rahl, P.B., and Young, R.A. (2009). SetDB1 contributes to repression of genes encoding developmental regulators and maintenance of ES cell state. Genes Dev *23*, 2484-2489.

Borger, D.R., Tanabe, K.K., Fan, K.C., Lopez, H.U., Fantin, V.R., Straley, K.S., Schenkein, D.P., Hezel, A.F., Ancukiewicz, M., Liebman, H.M., *et al.* (2012). Frequent mutation of isocitrate dehydrogenase (IDH)1 and IDH2 in cholangiocarcinoma identified through broad-based tumor genotyping. Oncologist *17*, 72-79.

Cai, L., Sutter, B.M., Li, B., and Tu, B.P. (2011). Acetyl-CoA induces cell growth and proliferation by promoting the acetylation of histones at growth genes. Mol Cell *42*, 426-437.

Cairns, R.A., Iqbal, J., Lemonnier, F., Kucuk, C., de Leval, L., Jais, J.P., Parrens, M., Martin, A., Xerri, L., Brousset, P., *et al.* (2012). IDH2 mutations are frequent in angioimmunoblastic T-cell lymphoma. Blood.

Ceol, C.J., Houvras, Y., Jane-Valbuena, J., Bilodeau, S., Orlando, D.A., Battisti, V., Fritsch, L., Lin, W.M., Hollmann, T.J., Ferre, F., *et al.* (2011). The histone methyltransferase SETDB1 is recurrently amplified in melanoma and accelerates its onset. Nature *471*, 513-517.

Chance, B., Estabrook, R.W., and Ghosh, A. (1964). Damped Sinusoidal Oscillations of Cytoplasmic Reduced Pyridine Nucleotide in Yeast Cells. Proc Natl Acad Sci U S A *51*, 1244-1251.

Chowdhury, R., Yeoh, K.K., Tian, Y.M., Hillringhaus, L., Bagg, E.A., Rose, N.R., Leung, I.K., Li, X.S., Woon, E.C., Yang, M., *et al.* (2011). The oncometabolite 2-hydroxyglutarate inhibits histone lysine demethylases. EMBO Rep *12*, 463-469.

Dang, L., White, D.W., Gross, S., Bennett, B.D., Bittinger, M.A., Driggers, E.M., Fantin, V.R., Jang, H.G., Jin, S., Keenan, M.C., *et al.* (2009). Cancer-associated IDH1 mutations produce 2-hydroxyglutarate. Nature *462*, 739-744.

Delhommeau, F., Dupont, S., Della Valle, V., James, C., Trannoy, S., Masse, A., Kosmider, O., Le Couedic, J.P., Robert, F., Alberdi, A., *et al.* (2009). Mutation in TET2 in myeloid cancers. N Engl J Med *360*, 2289-2301.

Fernandez, H.F., Sun, Z., Yao, X., Litzow, M.R., Luger, S.M., Paietta, E.M., Racevskis, J., Dewald, G.W., Ketterling, R.P., Bennett, J.M., *et al.* (2009). Anthracycline dose intensification in acute myeloid leukemia. N Engl J Med *361*, 1249-1259.

Figueroa, M.E., Abdel-Wahab, O., Lu, C., Ward, P.S., Patel, J., Shih, A., Li, Y., Bhagwat, N., Vasanthakumar, A., Fernandez, H.F., *et al.* (2010a). Leukemic IDH1 and IDH2 mutations result in a hypermethylation phenotype, disrupt TET2 function, and impair hematopoietic differentiation. Cancer Cell *18*, 553-567.

Figueroa, M.E., Lugthart, S., Li, Y., Erpelinck-Verschueren, C., Deng, X., Christos, P.J., Schifano, E., Booth, J., van Putten, W., Skrabanek, L., *et al.* (2010b). DNA methylation signatures identify biologically distinct subtypes in acute myeloid leukemia. Cancer Cell *17*, 13-27.

Figueroa, M.E., Wouters, B.J., Skrabanek, L., Glass, J., Li, Y., Erpelinck-Verschueren, C.A., Langerak, A.W., Lowenberg, B., Fazzari, M., Greally, J.M., *et al.* (2009). Genome-

wide epigenetic analysis delineates a biologically distinct immature acute leukemia with myeloid/T-lymphoid features. Blood *113*, 2795-2804.

Gumbiner, B.M. (2005). Regulation of cadherin-mediated adhesion in morphogenesis. Nat Rev Mol Cell Biol *6*, 622-634.

Habib, M., Fares, F., Bourgeois, C.A., Bella, C., Bernardino, J., Hernandez-Blazquez, F., de Capoa, A., and Niveleau, A. (1999). DNA global hypomethylation in EBV-transformed interphase nuclei. Exp Cell Res *249*, 46-53.

Hanahan, D., and Weinberg, R.A. (2011). Hallmarks of cancer: the next generation. Cell *144*, 646-674.

Hao, H.X., Khalimonchuk, O., Schraders, M., Dephoure, N., Bayley, J.P., Kunst, H., Devilee, P., Cremers, C.W., Schiffman, J.D., Bentz, B.G., *et al.* (2009). SDH5, a gene required for flavination of succinate dehydrogenase, is mutated in paraganglioma. Science *325*, 1139-1142.

He, Y.F., Li, B.Z., Li, Z., Liu, P., Wang, Y., Tang, Q., Ding, J., Jia, Y., Chen, Z., Li, L., *et al.* (2011). Tet-mediated formation of 5-carboxylcytosine and its excision by TDG in mammalian DNA. Science *333*, 1303-1307.

Hu, Z., Gomes, I., Horrigan, S.K., Kravarusic, J., Mar, B., Arbieva, Z., Chyna, B., Fulton, N., Edassery, S., Raza, A., *et al.* (2001). A novel nuclear protein, 5qNCA (LOC51780) is a candidate for the myeloid leukemia tumor suppressor gene on chromosome 5 band q31. Oncogene *20*, 6946-6954.

Huang, X., Holden, H.M., and Raushel, F.M. (2001). Channeling of substrates and intermediates in enzyme-catalyzed reactions. Annu Rev Biochem *70*, 149-180.

Ingvarsdottir, K., Edwards, C., Lee, M.G., Lee, J.S., Schultz, D.C., Shilatifard, A., Shiekhattar, R., and Berger, S.L. (2007). Histone H3 K4 demethylation during activation and attenuation of GAL1 transcription in Saccharomyces cerevisiae. Mol Cell Biol *27*, 7856-7864.

Isaacs, J.S., Jung, Y.J., Mole, D.R., Lee, S., Torres-Cabala, C., Chung, Y.L., Merino, M., Trepel, J., Zbar, B., Toro, J., *et al.* (2005). HIF overexpression correlates with biallelic loss of fumarate hydratase in renal cancer: novel role of fumarate in regulation of HIF stability. Cancer Cell *8*, 143-153.

Ito, S., D'Alessio, A.C., Taranova, O.V., Hong, K., Sowers, L.C., and Zhang, Y. (2010). Role of Tet proteins in 5mC to 5hmC conversion, ES-cell self-renewal and inner cell mass specification. Nature *466*, 1129-1133.

Katada, S., Imhof, A., and Sassone-Corsi, P. (2012). Connecting threads: epigenetics and metabolism. Cell *148*, 24-28.

Katoh, Y., Ikura, T., Hoshikawa, Y., Tashiro, S., Ito, T., Ohta, M., Kera, Y., Noda, T., and Igarashi, K. (2011). Methionine adenosyltransferase II serves as a transcriptional corepressor of Maf oncoprotein. Mol Cell *41*, 554-566.

Klevecz, R.R., Bolen, J., Forrest, G., and Murray, D.B. (2004). A genomewide oscillation in transcription gates DNA replication and cell cycle. Proc Natl Acad Sci U S A *101*, 1200-1205.

Klose, R.J., and Zhang, Y. (2007). Regulation of histone methylation by demethylimination and demethylation. Nat Rev Mol Cell Biol *8*, 307-318.

Koivunen, P., Lee, S., Duncan, C.G., Lopez, G., Lu, G., Ramkissoon, S., Losman, J.A., Joensuu, P., Bergmann, U., Gross, S.*, et al.* (2012). Transformation by the (R)-enantiomer of 2-hydroxyglutarate linked to EGLN activation. Nature *483*, 484-488.

Krivtsov, A.V., and Armstrong, S.A. (2007). MLL translocations, histone modifications and leukaemia stem-cell development. Nat Rev Cancer *7*, 823-833.

Laporte, D., Lebaudy, A., Sahin, A., Pinson, B., Ceschin, J., Daignan-Fornier, B., and Sagot, I. (2011). Metabolic status rather than cell cycle signals control quiescence entry and exit. J Cell Biol *192*, 949-957.

Latham, J.A., and Dent, S.Y. (2007). Cross-regulation of histone modifications. Nat Struct Mol Biol *14*, 1017-1024.

Liefke, R., Oswald, F., Alvarado, C., Ferres-Marco, D., Mittler, G., Rodriguez, P., Dominguez, M., and Borggrefe, T. (2010). Histone demethylase KDM5A is an integral part of the core Notch-RBP-J repressor complex. Genes Dev *24*, 590-601.

Locasale, J.W., Grassian, A.R., Melman, T., Lyssiotis, C.A., Mattaini, K.R., Bass, A.J., Heffron, G., Metallo, C.M., Muranen, T., Sharfi, H.*, et al.* (2011). Phosphoglycerate dehydrogenase diverts glycolytic flux and contributes to oncogenesis. Nat Genet *43*, 869-874.

Losman, J.A., Looper, R., Koivunen, P., Lee, S., Schneider, R.K., McMahon, C., Cowley, G., Root, D., Ebert, B.L., and Kaelin, W.G., Jr. (2013). (R)-2-Hydroxyglutarate Is Sufficient to Promote Leukemogenesis and Its Effects Are Reversible. Science.

Lu, C., Ward, P.S., Kapoor, G.S., Rohle, D., Turcan, S., Abdel-Wahab, O., Edwards, C.R., Khanin, R., Figueroa, M.E., Melnick, A.*, et al.* (2012). IDH mutation impairs histone demethylation and results in a block to cell differentiation. Nature.

MacDougald, O.A., and Lane, M.D. (1995). Transcriptional regulation of gene expression during adipocyte differentiation. Annu Rev Biochem *64*, 345-373.

Mardis, E.R., Ding, L., Dooling, D.J., Larson, D.E., McLellan, M.D., Chen, K., Koboldt, D.C., Fulton, R.S., Delehaunty, K.D., McGrath, S.D., *et al.* (2009). Recurring mutations found by sequencing an acute myeloid leukemia genome. N Engl J Med *361*, 1058-1066.

Mikami, Y., Ishii, Y., Watanabe, N., Shirakawa, T., Suzuki, S., Irie, S., Isokawa, K., and Honda, M.J. (2011). CD271/p75(NTR) inhibits the differentiation of mesenchymal stem cells into osteogenic, adipogenic, chondrogenic, and myogenic lineages. Stem Cells Dev *20*, 901-913.

Mohammad, H.P., and Baylin, S.B. (2010). Linking cell signaling and the epigenetic machinery. Nat Biotechnol *28*, 1033-1038.

Mullarky, E., Mattaini, K.R., Vander Heiden, M.G., Cantley, L.C., and Locasale, J.W. (2011). PHGDH amplification and altered glucose metabolism in human melanoma. Pigment Cell Melanoma Res *24*, 1112-1115.

Ng, S.S., Kavanagh, K.L., McDonough, M.A., Butler, D., Pilka, E.S., Lienard, B.M., Bray, J.E., Savitsky, P., Gileadi, O., von Delft, F., *et al.* (2007). Crystal structures of histone demethylase JMJD2A reveal basis for substrate specificity. Nature *448*, 87-91.

Niemann, S., and Muller, U. (2000). Mutations in SDHC cause autosomal dominant paraganglioma, type 3. Nat Genet *26*, 268-270.

Noushmehr, H., Weisenberger, D.J., Diefes, K., Phillips, H.S., Pujara, K., Berman, B.P., Pan, F., Pelloski, C.E., Sulman, E.P., Bhat, K.P., *et al.* (2010). Identification of a CpG island methylator phenotype that defines a distinct subgroup of glioma. Cancer Cell *17*, 510-522.

Oermann, E.K., Wu, J., Guan, K.L., and Xiong, Y. (2012). Alterations of metabolic genes and metabolites in cancer. Semin Cell Dev Biol *23*, 370-380.

Ohm, J.E., McGarvey, K.M., Yu, X., Cheng, L., Schuebel, K.E., Cope, L., Mohammad, H.P., Chen, W., Daniel, V.C., Yu, W., *et al.* (2007). A stem cell-like chromatin pattern may predispose tumor suppressor genes to DNA hypermethylation and heritable silencing. Nat Genet *39*, 237-242.

Pansuriya, T.C., van Eijk, R., d'Adamo, P., van Ruler, M.A., Kuijjer, M.L., Oosting, J., Cleton-Jansen, A.M., van Oosterwijk, J.G., Verbeke, S.L., Meijer, D., *et al.* (2011). Somatic mosaic IDH1 and IDH2 mutations are associated with enchondroma and spindle cell hemangioma in Ollier disease and Maffucci syndrome. Nat Genet *43*, 1256-1261.

Parsons, D.W., Jones, S., Zhang, X., Lin, J.C., Leary, R.J., Angenendt, P., Mankoo, P., Carter, H., Siu, I.M., Gallia, G.L., *et al.* (2008). An integrated genomic analysis of human glioblastoma multiforme. Science *321*, 1807-1812.

Paschka, P., Schlenk, R.F., Gaidzik, V.I., Habdank, M., Kronke, J., Bullinger, L., Spath, D., Kayser, S., Zucknick, M., Gotze, K., *et al.* (2010). IDH1 and IDH2 mutations are frequent genetic alterations in acute myeloid leukemia and confer adverse prognosis in cytogenetically normal acute myeloid leukemia with NPM1 mutation without FLT3 internal tandem duplication. J Clin Oncol *28*, 3636-3643.

Possemato, R., Marks, K.M., Shaul, Y.D., Pacold, M.E., Kim, D., Birsoy, K., Sethumadhavan, S., Woo, H.K., Jang, H.G., Jha, A.K., *et al.* (2011). Functional genomics reveal that the serine synthesis pathway is essential in breast cancer. Nature *476*, 346-350.

Reznikoff, C.A., Brankow, D.W., and Heidelberger, C. (1973). Establishment and characterization of a cloned line of C3H mouse embryo cells sensitive to postconfluence inhibition of division. Cancer Res *33*, 3231-3238.

Sahar, S., and Sassone-Corsi, P. (2012). Regulation of metabolism: the circadian clock dictates the time. Trends Endocrinol Metab *23*, 1-8.

Sasaki, M., Knobbe, C.B., Itsumi, M., Elia, A.J., Harris, I.S., Chio, II, Cairns, R.A., McCracken, S., Wakeham, A., Haight, J., *et al.* (2012a). D-2-hydroxyglutarate produced by mutant IDH1 perturbs collagen maturation and basement membrane function. Genes Dev *26*, 2038-2049.

Sasaki, M., Knobbe, C.B., Munger, J.C., Lind, E.F., Brenner, D., Brustle, A., Harris, I.S., Holmes, R., Wakeham, A., Haight, J., *et al.* (2012b). IDH1(R132H) mutation increases murine haematopoietic progenitors and alters epigenetics. Nature *488*, 656-659.

Schwartzentruber, J., Korshunov, A., Liu, X.Y., Jones, D.T., Pfaff, E., Jacob, K., Sturm, D., Fontebasso, A.M., Quang, D.A., Tonjes, M., *et al.* (2012). Driver mutations in histone H3.3 and chromatin remodelling genes in paediatric glioblastoma. Nature *482*, 226-231.

Selak, M.A., Armour, S.M., MacKenzie, E.D., Boulahbel, H., Watson, D.G., Mansfield, K.D., Pan, Y., Simon, M.C., Thompson, C.B., and Gottlieb, E. (2005). Succinate links TCA cycle dysfunction to oncogenesis by inhibiting HIF-alpha prolyl hydroxylase. Cancer Cell *7*, 77-85.

Shyh-Chang, N., Locasale, J.W., Lyssiotis, C.A., Zheng, Y., Teo, R.Y., Ratanasirintrawoot, S., Zhang, J., Onder, T., Unternaehrer, J.J., Zhu, H., *et al.* (2013). Influence of threonine metabolism on S-adenosylmethionine and histone methylation. Science *339*, 222-226.

Slavov, N., Macinskas, J., Caudy, A., and Botstein, D. (2011). Metabolic cycling without cell division cycling in respiring yeast. Proc Natl Acad Sci U S A *108*, 19090-19095.

Song, L., Prey, J.D., Xue, J., Kanter, P., Manzotti, C., Bombardelli, E., Morazzoni, P., and Pendyala, L. (2005). Pharmacokinetic measurements of IDN 5390 using electrospray

ionization tandem mass spectrometry: structure characterization and quantification in dog plasma. Rapid Commun Mass Spectrom *19*, 3617-3625.

Strahl, B.D., and Allis, C.D. (2000). The language of covalent histone modifications. Nature *403*, 41-45.

Tahiliani, M., Koh, K.P., Shen, Y., Pastor, W.A., Bandukwala, H., Brudno, Y., Agarwal, S., Iyer, L.M., Liu, D.R., Aravind, L.*, et al.* (2009). Conversion of 5-methylcytosine to 5-hydroxymethylcytosine in mammalian DNA by MLL partner TET1. Science *324*, 930-935.

Taylor, S.M., and Jones, P.A. (1979). Multiple new phenotypes induced in 10T1/2 and 3T3 cells treated with 5-azacytidine. Cell *17*, 771-779.

Tefferi, A., Lasho, T.L., Abdel-Wahab, O., Guglielmelli, P., Patel, J., Caramazza, D., Pieri, L., Finke, C.M., Kilpivaara, O., Wadleigh, M.*, et al.* (2010). IDH1 and IDH2 mutation studies in 1473 patients with chronic-, fibrotic- or blast-phase essential thrombocythemia, polycythemia vera or myelofibrosis. Leukemia *24*, 1302-1309.

Tomlinson, I.P., Alam, N.A., Rowan, A.J., Barclay, E., Jaeger, E.E., Kelsell, D., Leigh, I., Gorman, P., Lamlum, H., Rahman, S.*, et al.* (2002). Germline mutations in FH predispose to dominantly inherited uterine fibroids, skin leiomyomata and papillary renal cell cancer. Nat Genet *30*, 406-410.

Tristan, C., Shahani, N., Sedlak, T.W., and Sawa, A. (2011). The diverse functions of GAPDH: Views from different subcellular compartments. Cellular Signalling *23*, 317-323.

Tsukada, Y., Fang, J., Erdjument-Bromage, H., Warren, M.E., Borchers, C.H., Tempst, P., and Zhang, Y. (2006). Histone demethylation by a family of JmjC domain-containing proteins. Nature *439*, 811-816.

Tu, B.P., Kudlicki, A., Rowicka, M., and McKnight, S.L. (2005). Logic of the yeast metabolic cycle: temporal compartmentalization of cellular processes. Science *310*, 1152-1158.

Tu, B.P., and McKnight, S.L. (2009). Evidence of carbon monoxide-mediated phase advancement of the yeast metabolic cycle. Proc Natl Acad Sci U S A *106*, 14293-14296.

Tu, B.P., Mohler, R.E., Liu, J.C., Dombek, K.M., Young, E.T., Synovec, R.E., and McKnight, S.L. (2007). Cyclic changes in metabolic state during the life of a yeast cell. Proc Natl Acad Sci U S A *104*, 16886-16891.

Turcan, S., Rohle, D., Goenka, A., Walsh, L.A., Fang, F., Yilmaz, E., Campos, C., Fabius, A.W., Lu, C., Ward, P.S.*, et al.* (2012). IDH1 mutation is sufficient to establish the glioma hypermethylator phenotype. Nature *483*, 479-483.

Ulanovskaya, O.A., Zuhl, A.M., and Cravatt, B.F. (2013). NNMT promotes epigenetic remodeling in cancer by creating a metabolic methylation sink. Nat Chem Biol.

van Haaften, G., Dalgliesh, G.L., Davies, H., Chen, L., Bignell, G., Greenman, C., Edkins, S., Hardy, C., O'Meara, S., Teague, J., *et al.* (2009). Somatic mutations of the histone H3K27 demethylase gene UTX in human cancer. Nat Genet *41*, 521-523.

Vander Heiden, M.G., Cantley, L.C., and Thompson, C.B. (2009). Understanding the Warburg effect: the metabolic requirements of cell proliferation. Science *324*, 1029-1033.

Verhaak, R.G., Hoadley, K.A., Purdom, E., Wang, V., Qi, Y., Wilkerson, M.D., Miller, C.R., Ding, L., Golub, T., Mesirov, J.P., *et al.* (2010). Integrated genomic analysis identifies clinically relevant subtypes of glioblastoma characterized by abnormalities in PDGFRA, IDH1, EGFR, and NF1. Cancer Cell *17*, 98-110.

Wang, J., Alexander, P., Wu, L., Hammer, R., Cleaver, O., and McKnight, S.L. (2009). Dependence of mouse embryonic stem cells on threonine catabolism. Science *325*, 435-439.

Wang, P., Dong, Q., Zhang, C., Kuan, P.F., Liu, Y., Jeck, W.R., Andersen, J.B., Jiang, W., Savich, G.L., Tan, T.X., *et al.* (2012). Mutations in isocitrate dehydrogenase 1 and 2 occur frequently in intrahepatic cholangiocarcinomas and share hypermethylation targets with glioblastomas. Oncogene.

Warburg, O. (1956). On the origin of cancer cells. Science *123*, 309-314.

Ward, P.S., Cross, J.R., Lu, C., Weigert, O., Abel-Wahab, O., Levine, R.L., Weinstock, D.M., Sharp, K.A., and Thompson, C.B. (2012). Identification of additional IDH mutations associated with oncometabolite R(-)-2-hydroxyglutarate production. Oncogene *31*, 2491-2498.

Ward, P.S., Patel, J., Wise, D.R., Abdel-Wahab, O., Bennett, B.D., Coller, H.A., Cross, J.R., Fantin, V.R., Hedvat, C.V., Perl, A.E., *et al.* (2010). The common feature of leukemia-associated IDH1 and IDH2 mutations is a neomorphic enzyme activity converting alpha-ketoglutarate to 2-hydroxyglutarate. Cancer Cell *17*, 225-234.

Ward, P.S., and Thompson, C.B. (2012). Metabolic reprogramming: a cancer hallmark even warburg did not anticipate. Cancer Cell *21*, 297-308.

Wellen, K.E., Hatzivassiliou, G., Sachdeva, U.M., Bui, T.V., Cross, J.R., and Thompson, C.B. (2009). ATP-citrate lyase links cellular metabolism to histone acetylation. Science *324*, 1076-1080.

Widschwendter, M., Fiegl, H., Egle, D., Mueller-Holzner, E., Spizzo, G., Marth, C., Weisenberger, D.J., Campan, M., Young, J., Jacobs, I., *et al.* (2007). Epigenetic stem cell signature in cancer. Nat Genet *39*, 157-158.

Williams, K., Christensen, J., and Helin, K. (2012). DNA methylation: TET proteins-guardians of CpG islands? EMBO Rep *13*, 28-35.

Wu, G., Broniscer, A., McEachron, T.A., Lu, C., Paugh, B.S., Becksfort, J., Qu, C., Ding, L., Huether, R., Parker, M.*, et al.* (2012). Somatic histone H3 alterations in pediatric diffuse intrinsic pontine gliomas and non-brainstem glioblastomas. Nat Genet *44*, 251-253.

Wu, H., and Zhang, Y. (2011). Tet1 and 5-hydroxymethylation A genome-wide view in mouse embryonic stem cells. Cell Cycle *10*, 2428-2436.

Xiao, M., Yang, H., Xu, W., Ma, S., Lin, H., Zhu, H., Liu, L., Liu, Y., Yang, C., Xu, Y.*, et al.* (2012). Inhibition of alpha-KG-dependent histone and DNA demethylases by fumarate and succinate that are accumulated in mutations of FH and SDH tumor suppressors. Genes Dev *26*, 1326-1338.

Xu, W., Yang, H., Liu, Y., Yang, Y., Wang, P., Kim, S.H., Ito, S., Yang, C., Xiao, M.T., Liu, L.X.*, et al.* (2011). Oncometabolite 2-hydroxyglutarate is a competitive inhibitor of alpha-ketoglutarate-dependent dioxygenases. Cancer Cell *19*, 17-30.

Yamane, K., Toumazou, C., Tsukada, Y., Erdjument-Bromage, H., Tempst, P., Wong, J., and Zhang, Y. (2006). JHDM2A, a JmjC-containing H3K9 demethylase, facilitates transcription activation by androgen receptor. Cell *125*, 483-495.

Yan, H., Parsons, D.W., Jin, G., McLendon, R., Rasheed, B.A., Yuan, W., Kos, I., Batinic-Haberle, I., Jones, S., Riggins, G.J.*, et al.* (2009). IDH1 and IDH2 mutations in gliomas. N Engl J Med *360*, 765-773.

Yang, W., Xia, Y., Ji, H., Zheng, Y., Liang, J., Huang, W., Gao, X., Aldape, K., and Lu, Z. (2011). Nuclear PKM2 regulates beta-catenin transactivation upon EGFR activation. Nature *480*, 118-122.

Zhao, S., Lin, Y., Xu, W., Jiang, W., Zha, Z., Wang, P., Yu, W., Li, Z., Gong, L., Peng, Y.*, et al.* (2009). Glioma-derived mutations in IDH1 dominantly inhibit IDH1 catalytic activity and induce HIF-1alpha. Science *324*, 261-265.